27
5-9-77

SAND77-0380

Unlimited Release

3151

# Solar Irrigation Program - Status Report October 1976 through January 1977

Robert L. Alvis

Prepared by Sandia Laboratories, Albuquerque, New Mexico 87115 and Livermore, California 94550 for the United States Energy Research and Development Administration under Contract AT(29–1)-789

Printed April 1977

Sandia Laboratories

SF 2900 Q(7-73)

MASTER

## DISCLAIMER

Issued by Sandia Laboratories, operated for the United States Energy Research & Development Administration by Sandia Corporation.

**NOTICE**



Printed in the United States of America

Available from
National Technical Information Service
U. S. Department of Commerce
5285 Port Royal Road
Springfield, VA 22161

Price: Printed Copy $4.50 ; Microfiche $3.00

SAND77-0380
Unlimited Release
Printed April 1977

# SOLAR IRRIGATION PROGRAM - STATUS REPORT
## October 1976 through January 1977

Submitted to

ENERGY RESEARCH AND DEVELOPMENT AGENCY
DIVISION OF SOLAR ENERGY

Robert L. Alvis
Advanced Energy Projects 5715
Sandia Laboratories
Albuquerque, NM 87115



## ABSTRACT

This report documents the status of the Solar Irrigation Program. The program initially consisted of a shallow well experiment that is now under construction in New Mexico. It has recently been expanded to include a deep well experiment in Arizona and a follow-on, as yet undefined, demonstration system. Most of this report is limited to technical discussions of the shallow well experiment design, and analyses are given which support the design choices selected.

ACKNOWLEDGMENT

This report includes the work of several laboratory personnel. Their effort and their work has been of significant aid to the design and understanding of the technologies involved. Topics in which another co-worker has significantly contributed has been noted by giving this person's name at the beginning of the topic.

CONTENTS

FIGURES

FIGURES (cont)



TABLES

SOLAR IRRIGATION PROGRAM - STATUS REPORT

## Introduction

This report documents the progress made by the Solar Irrigation Project during the period October 1976 through January 1977. The preceding report[1] gave a general description of the ERDA/New Mexico solar irrigation experiment. Since issuance of that report, ERDA has expanded the program.[2] This report will describe the status of the expanded solar irrigation program.

Several supportive reasons for having a solar irrigation program have previously been discussed. These reasons are still valid, and many are becoming more acute. For instance, in 1974 our petroleum imports approximately equaled our agricultural exports as illustrated in Figure 1. In 1975 the petroleum imports increased to $35 billion--a rate of growth that is certain to become unacceptable. A large amount of energy is consumed by irrigation. The water pumped for irrigation in the United States during 1974 consumed 80 billion kW-hr. Since an average home consumes an equivalent of approximately 17,000 kW-hr per year, this means that 5 million homes could be heated with this energy as illustrated in Figure 2, so one can easily predict where the energy will be distributed in event of a shortage.

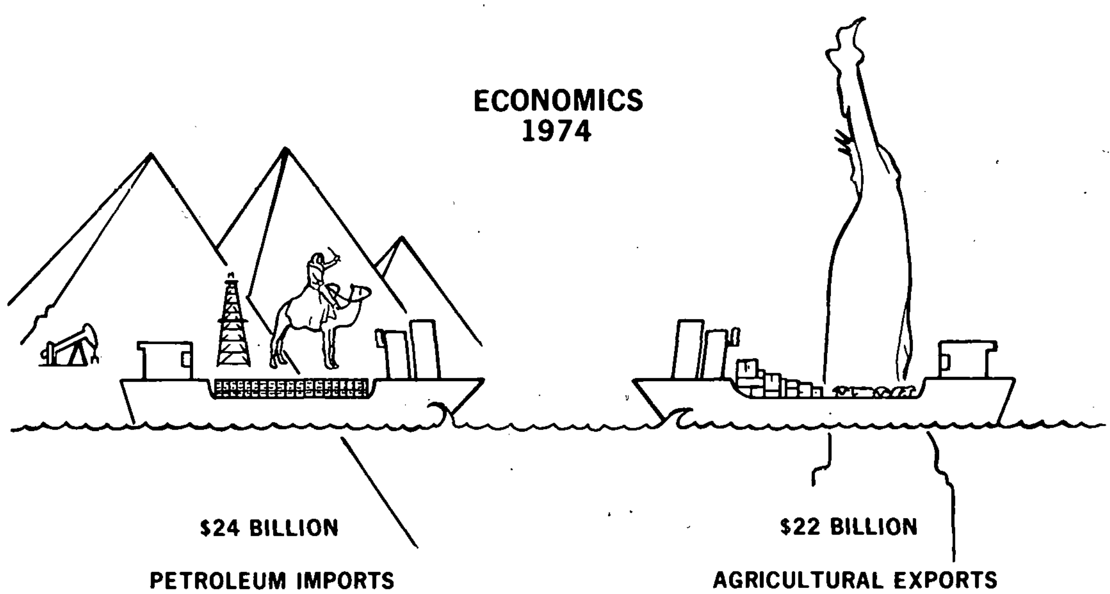


Figure 1. Petroleum Imports versus Agricultural Exports

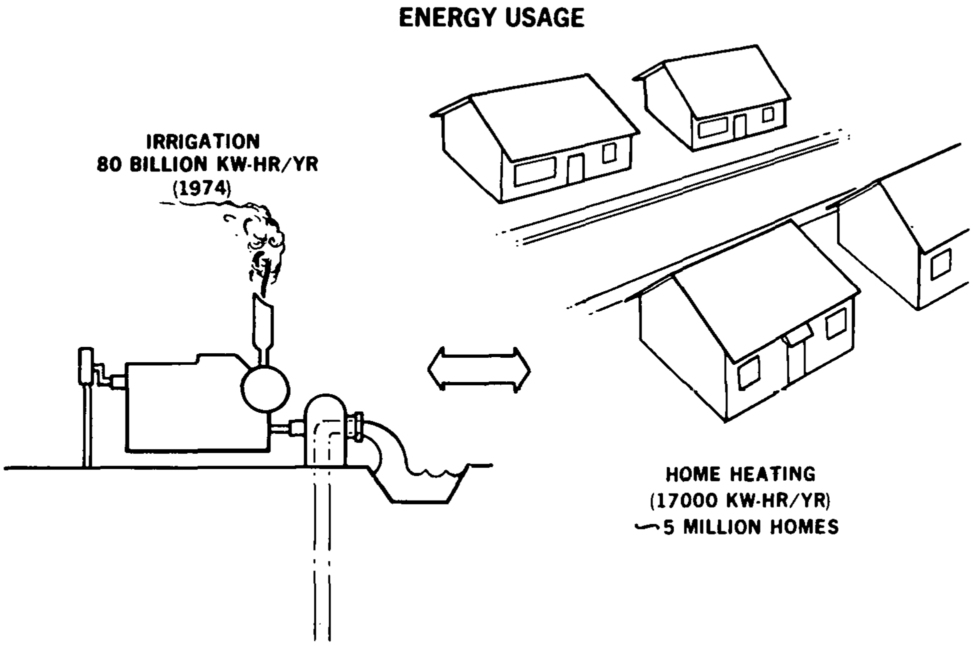


Figure 2. Energy Use Comparison

Irrigation is important; twenty percent of all farm sales in the United States in 1969 were for crops from irrigated farms.[3] Most of the country's irrigation is conducted in areas of high insolation and therefore, solar energy for irrigation has the potential to be an alternate to fossil fuel and aid in increasing crop production.

The cost of fossil fuel has rapidly increased for the farmer. This improves the economic feasibility of solar energy. The cost of electricity for central New Mexico farmers increased from $0.02/kW-hr to $0.04/kW-hr on November 1, 1976. Natural gas also increased in 1976 to $1.40/mcf and is predicted to increase to $5.00/mcf by 1982. No irrigation customers are assured that they can obtain either type of energy in the future. With this uncertainty about energy and the present high production cost to crop value ratio, many farmers are under financial stress and asking for assistance.

## Solar Irrigation Program

A solar irrigation program plan has been formulated for ERDA. It has been published and has been distributed for comment.[2] The following is a summary of the plan (Figure 3).

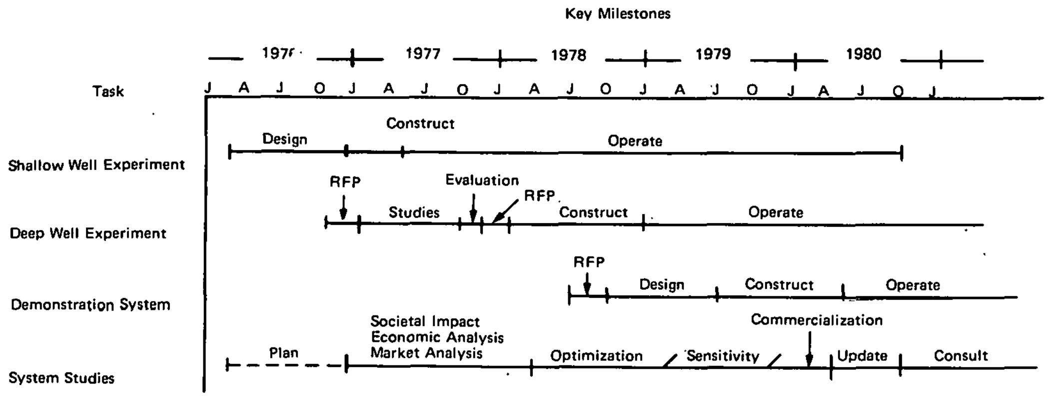


Figure 3. Solar Irrigation Program Activities Schedule

## Program Objectives

The objectives of this program are to determine if solar energy can economically become an alternative for fossil energy in powering irrigation pumps, demonstrate the performance of developed systems, and implement the commercialization of the system.

## Program Approach

The approach is to conduct design studies, construct experiments to obtain performance and cost data to confirm design studies, and to utilize this data in system studies to determine what regions of our nation the system can best be used and what incentives are needed to insure that a solar energy system design is available which can be successfully implemented by commercial firms to power irrigation pumps.

The approach will include the following major tasks:

### Shallow Well Experiment

A shallow well experiment will be conducted in conjunction with the State of New Mexico. This experiment has been restricted to a temperature below 600°F and will produce approximately 19 kW (25 hp). This will allow the use of inexpensive components, but the system will be penalized by moderate thermodynamic efficiency. The results of this experiment will determine the performance that can be expected from this type of design. Performance is the amount of energy delivered per unit system cost. Agricultural experiments will be conducted by New Mexico State University as a part of this experiment to determine the most efficient use of the water pumped.

Deep Well Experiment

A deep well experiment will be conducted in conjunction with the State of Arizona. This experiment design has been restricted to operating temperature of 600 °F or higher and shall produce 150 $kW_e$ (200 hp). Plans are to award three study contracts to industry to study selected proposals for the system. The results of the studies will indicate which design approach has the economic and technical potential for being commercialized. Depending upon the study results, one of the designs will be built in Southern Arizona. The University of Arizona will conduct agricultural experiments to determine the most efficient use of the water pumped for that region of the nation.

Demonstration System

A demonstration solar irrigation system is planned to be a follow-on to the two experiments. Its design will be dependent upon the experimental units and will incorporate all concepts of the previous experiments which demonstrated high performance per unit cost. The site, size and concept used will be chosen to demonstrate to the agricultural and financial communities that solar irrigation is a viable alternative to fossil fuel powered systems.

System Studies

A system study is being done as a task of the overall program to identify and assess the market requirement so the system can become a practical alternative to conventional power sources. This study will assess regional and national market potential, the number of design concepts required, and the commercialization required to get solar systems operating on privately owned farms and ranches.

Expected Results

The shallow well experiment task will provide actual performance versus cost data on a medium temperature design concept. System studies will utilize this data as well as a system design to determine the "best" design which industry could market. The deep well experiment will determine the maximum performance versus cost data of a high temperature solar irrigation system. The data from these two experiments will give design direction to the demonstration unit. The demonstration unit will include all the technology learned which will lead to high performance and low cost. The demonstration unit, with the systems studies, will show the public how and where solar irrigation can be an alternative to conventional irrigation power sources. With this information and assistance from ERDA, solar irrigation is expected to become a marketable product by commercial firms.

Sandia Laboratories have been appointed technical director for ERDA's solar irrigation program in addition to the project effort with New Mexico State University on the ERDA/New Mexico experiment. As technical director we have aided ERDA-ALO in writing the Request for Proposal (RFP) for the deep well experiment and have reviewed twenty-one proposals they received for technical content. Recommendations regarding the proposals have been made to ERDA. ERDA is planning to award the study portion of the deep well experiment by February 1, 1977.

## ERDA/New Mexico Experiment

The ERDA/New Mexico experiment is a shallow well experiment to be conducted in the Estancia Valley of New Mexico. The site selected for the experiment is the Torrance County Land and Livestock Company farm near Willard, New Mexico.[4] A layout of the farm is shown in Figure 4. It can be seen that the experiment will be constructed on the corner of a field that is missed by a center-pivot irrigation system and the experimental field to be farmed is across the road to the north.

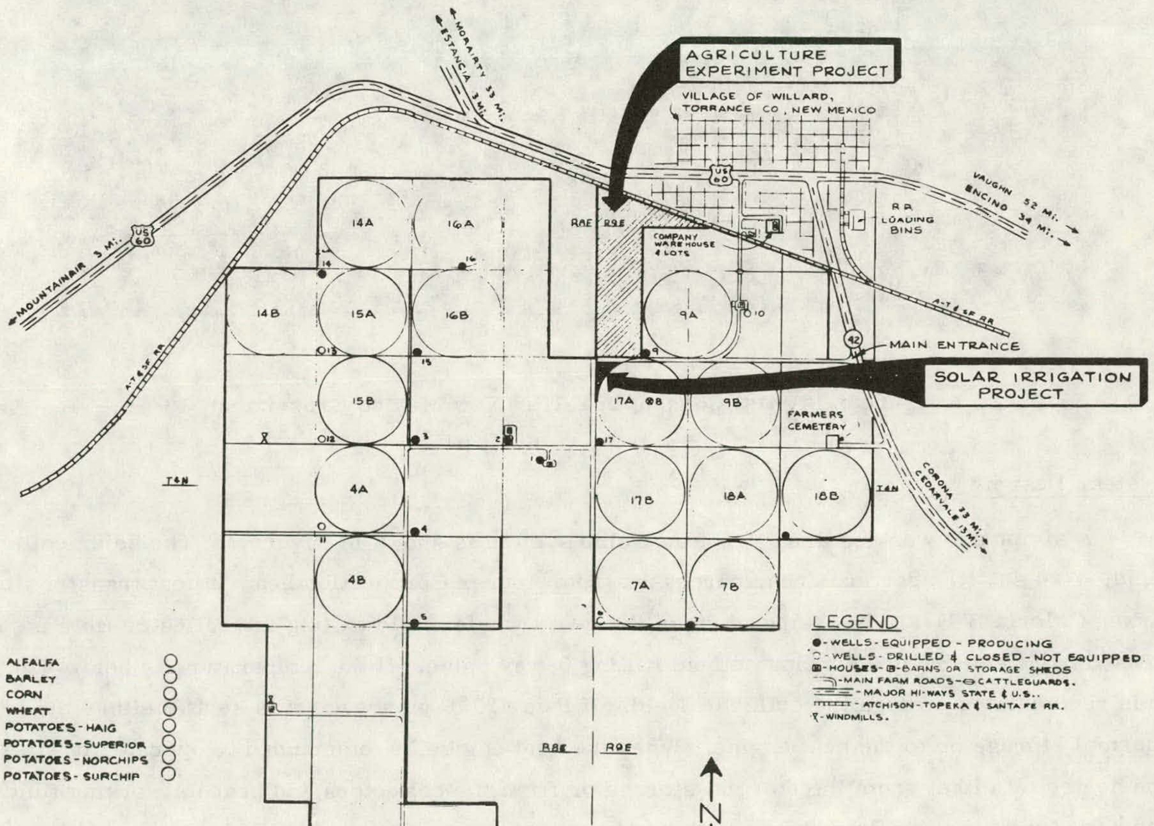


Figure 4. ERDA/New Mexico Experiment Site

The artist's concept of the experiment, drawn very closely to the design definition, is shown in Figure 5. Construction has begun as can be seen in Figure 6. Construction is approximately one month behind schedule due to unseasonally poor weather during the month of November. Little construction was planned for December and January; therefore, this time will be used to get back on schedule. The equipment is expected to be in operation by May 1, 1977.

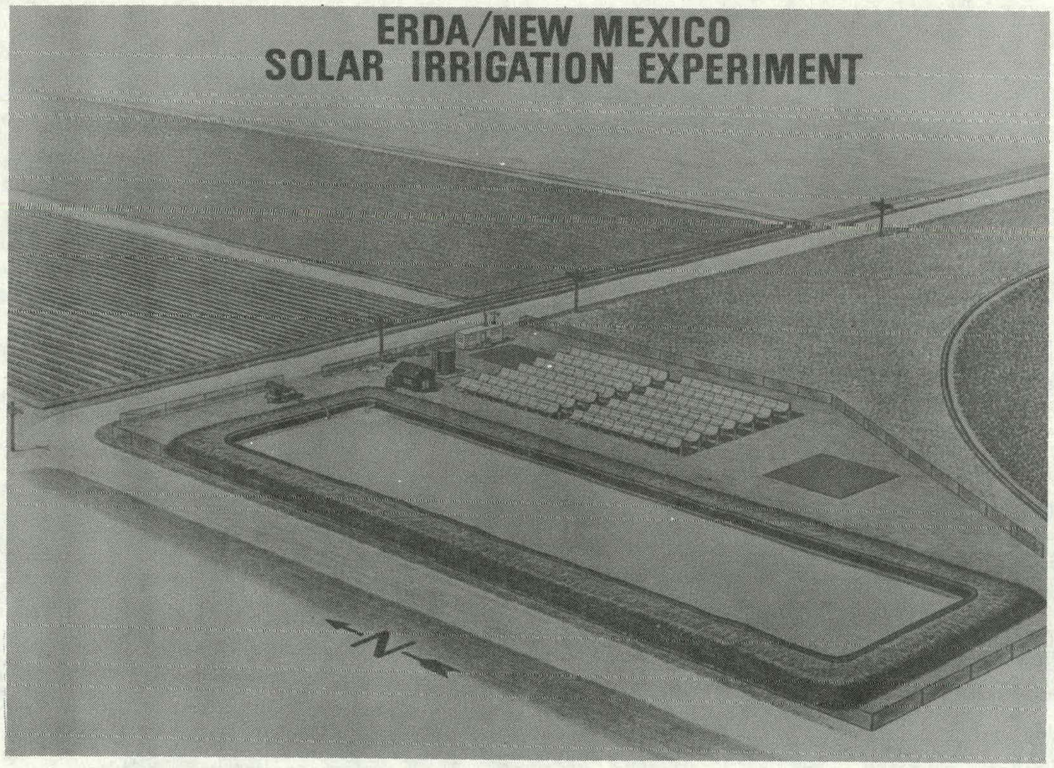


Figure 5. Artist Concept of ERDA/New Mexico Experiment

System Design

A simplified working diagram of the solar system is shown in Figure 7. The solar collector field, 6720 sq. ft. aperture area, purchased from Acurex Corporation heats a heat transfer fluid, Exxon Caloria HT43. The temperature of the heat transfer fluid exiting the collector field is sensed by a temperature sensing self-activating 3-way valve. If the temperature is below 420 °F, it is recirculated through the collector field. If it is 420 °F or above, it is sent to either the thermal storage or to the heat engine. When the heat engine is commanded to operate, it will take the heated oil either from the thermal storage or from the collectors and heat its working fluid by the use of a boiler and fluid pump. Another temperature sensing self-activating 2-way valve on the outlet of the boiler will only allow 240 °F or lower temperature fluid to return to the thermal storage reservoir. The working fluid (R-113) is expanded through a turbine. A regenerator is included for improved cycle efficiency. The condenser returns the working fluid to the liquid state before being returned to the regenerator and boiler. The boiler, turbine, regenerator, condenser and associated pumps are considered as parts of the heat engine. The heat engine is being supplied by Barber-Nichols Engineering Co.

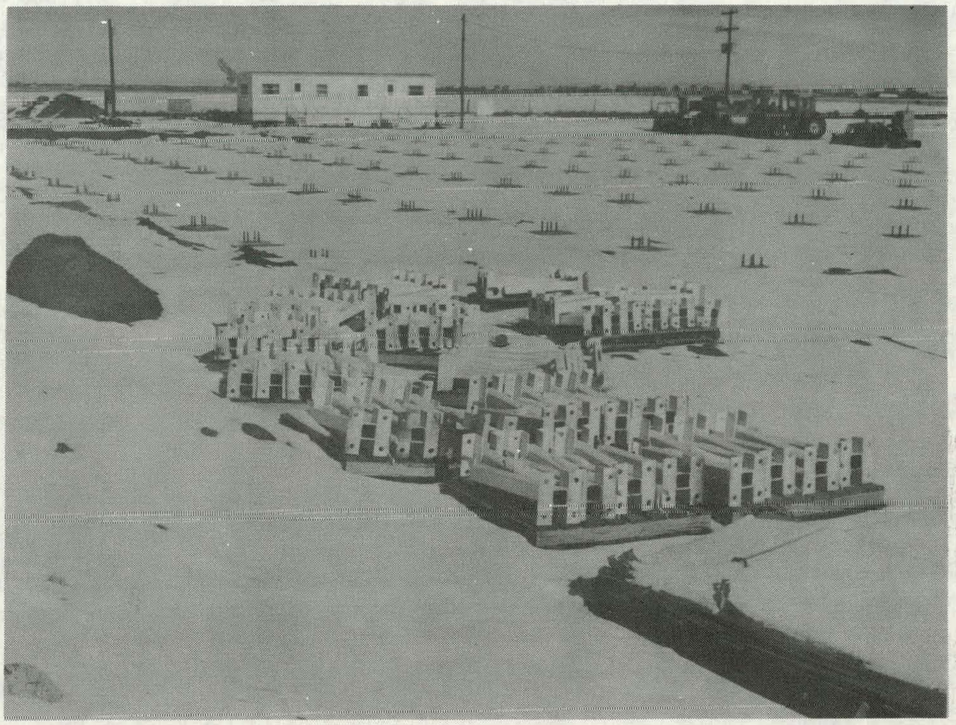

Figure 6. Photograph of Experiment Construction, January 7, 1977

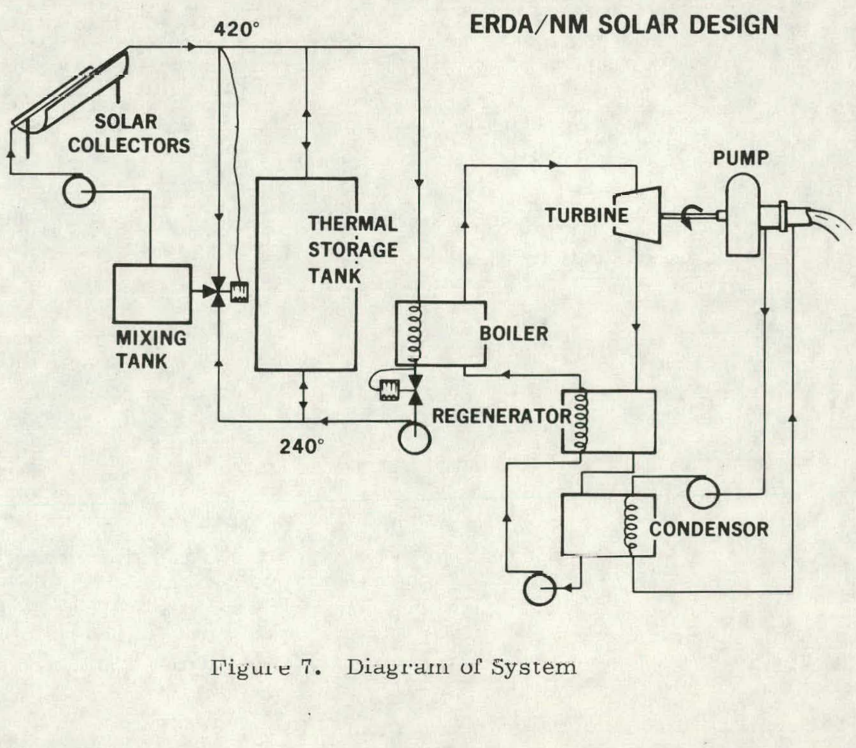


Figure 7. Diagram of System

Design changes have been approved on the heat engine to allow ball bearings to be used in place of dynamic bearings. This change will require the bearings to be replaced after three years of operation, but the engine will produce 26 hp instead of 25 hp. The additional power was considered worth the change.

A water circulation pump had to be added to the condenser. Throttling the pumped water required approximately 2 hp additional power from the engine where the pump requires approximately 1/2 hp. The engine is being fitted with instrumentation for data acquisition. This includes working fluid temperature and flow, torque produced and shaft rotation speed.

Heat Transfer Fluid Control System (A. F. Veneruso)

Figure 8 is a simplified block diagram which shows major elements of the solar powered irrigation system. The heat transfer fluid, Caloria HT43, is pumped by the fixed displacement, constant speed pump into the solar collectors where it is heated to 215°C (420°F). The three-way valve controls the collectors' outlet temperature by recirculating part or all of the heat transfer fluid back through the solar collectors. The control valve functions continuously with a variable duty cycle to accommodate changes in the solar collector's inlet temperature as well as changes in solar insolation. The buffer tank smooths out temperature transients and slows down the valve's switching rate.

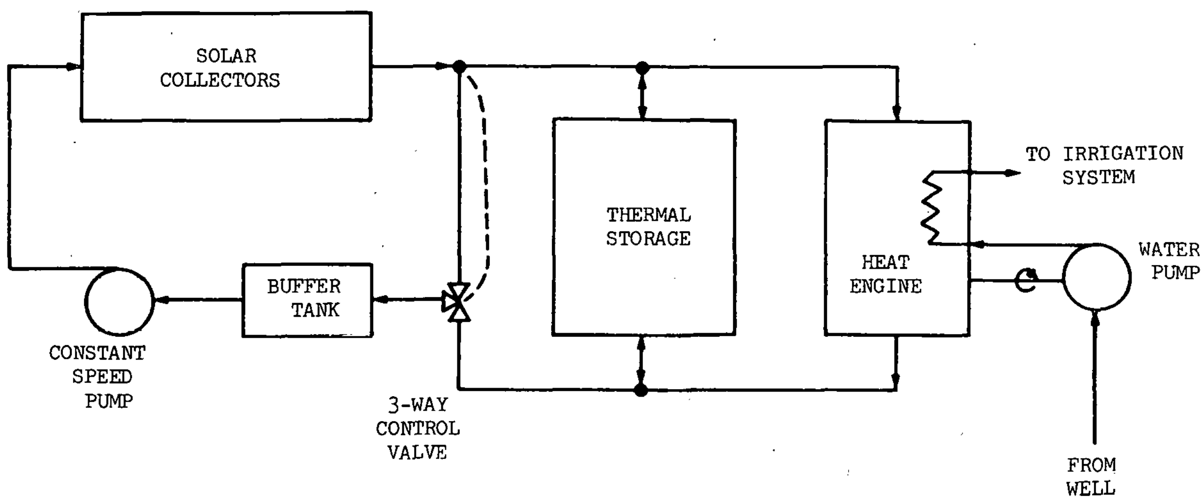


Figure 8. Control System Simplified Block Diagram

When the system is in operation, heat transfer fluid of the proper temperature is sent to thermal storage; and if the heat engine is running, it electrically pumps its own required hot fluid either from storage or directly from the solar collectors. Thermal storage is included in this system to effectively utilize daily variations in solar insolation while running the heat engine at a fixed speed, optimum efficiency condition.

The self-actuating, vapor pressure operated, three-way valve is the key temperature control element in this system. To illustrate the basic operation of this commercially available valve, a simplified drawing of its key parts is shown in Figure 9. The valve's sensing bulb is placed in thermal contact with the working fluid whose temperature is being controlled. The vapor pressure of the volatile fluid in the sensing bulb acts on a diaphragm in the pressure chamber and presses down on the actuating rod and restoring spring. If the sensing bulb's temperature is sufficiently high, the vapor pressure will be high enough to overcome the valve spring force and depress the actuating rod so that the valve disc closes off port L and allows fluid to flow between ports U and C. If, on the other hand, the sensing bulb's temperature is low, the corresponding vapor pressure is also low and the restoring spring raises the actuating rod and the valve disc closes off port U and allows flow between ports L and C. The valve's temperature control range and switchover point are set by selection of the volatile fluid and by adjustment of the spring force.

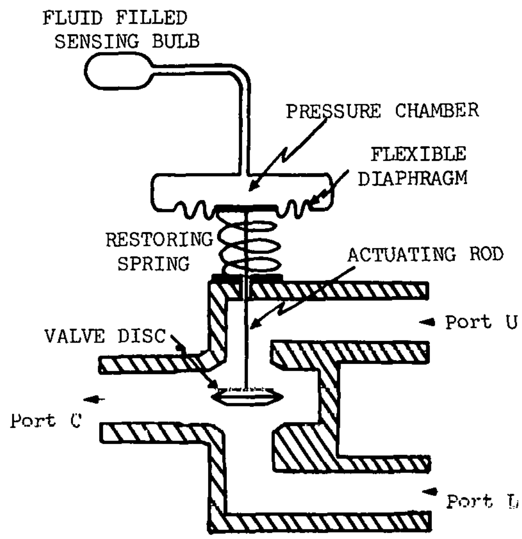


Figure 9. Control Valve Working Diagram

The valve selected for use in this Solar Irrigation Project is a 36RY517-23 3-way, self-actuating temperature control valve made by the Taylor Instrument Process Control Division of the Sybron Corporation in Rochester, New York. The complete valve, including the self-actuating temperature adjustable controller with a stainless steel bulb on a ten foot flexible extension, costs approximately $750.

In its application to the solar powered irrigation system, illustrated in Figure 10, the 3-way valve is placed in the return line from storage and the heat engine so that hot fluid from the solar collectors can be recirculated. The sensing bulb is placed in a "tee" at the solar collector's outlet. This placement offers a number of advantages over the alternative arrangement, shown in Figure 11, that was first studied for this project. Among the advantages of the placement shown in Figure 10 over that of Figure 11 are:

1) The valve runs cooler thus extending it life
2) The plumbing is simpler
3) The "sneak" flow path illustrated in Figure 11 is eliminated
4) There is a better mixing of the fluid returned to the collectors through the Buffer Tank.

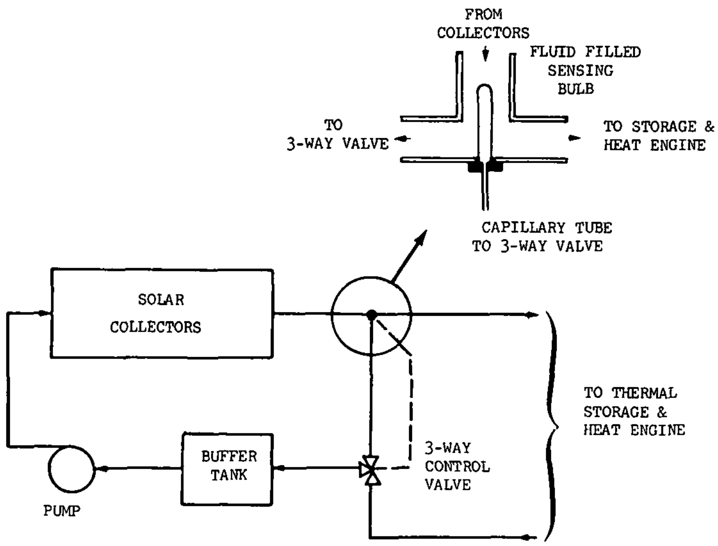


Figure 10. Fluid Control System Schematic

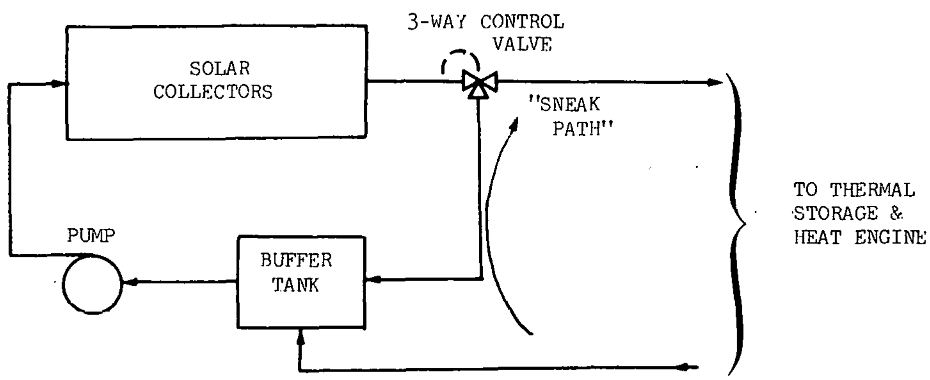


Figure 11. Alternate 3-Way Valve Control Arrangement

In its operation with the rest of the solar irrigation system, the 3-way valve has three modes of operation: recirculation, mixing and output. If, as shown in Figure 12a, the fluid's temperature, $T_{out}$, leaving the solar collectors is less than the lower control temperature, $T_L$, the valve recirculates the fluid back through the collectors for reheating. Figure 12b shows the case where the fluid temperature from the collectors is greater than $T_L$, but less than the high control temperature, $T_H$. In this case the valve mixes some lower temperature return fluid with some hot fluid from the solar collectors. In the output mode, shown in Figure 12c, the outlet temperature is hotter than $T_H$ and the hot fluid flows directly to storage or to the heat engine while the lower temperature return fluid flows directly back to the solar collectors.

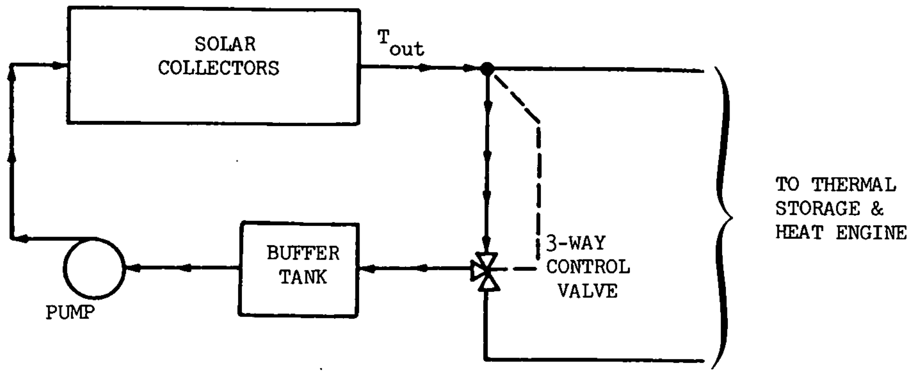


a) Recirculating Mode - Fluid Cold

$T_{out} < T_L$

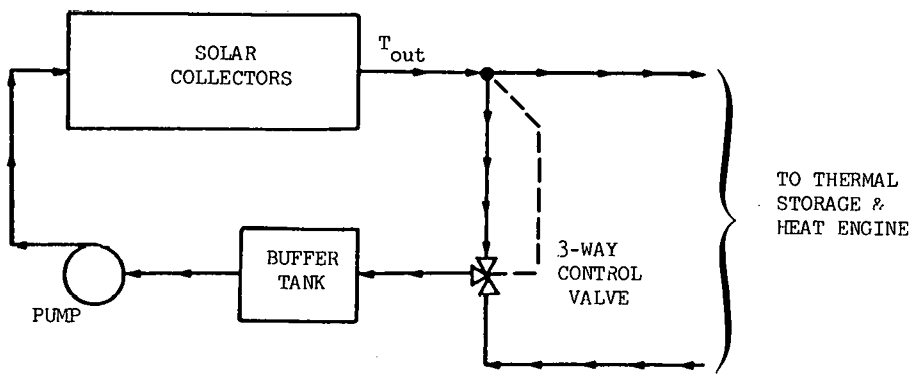


b) Mixing Mode - Fluid Warm

$T_L < T_{out} < T_H$

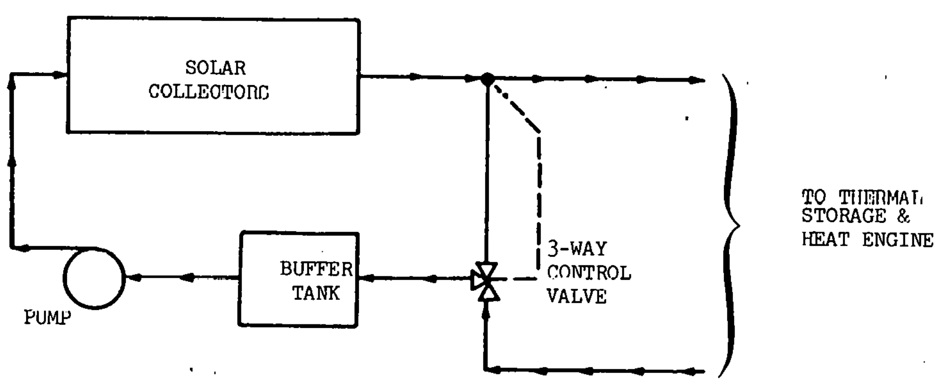


c) Output Mode - Fluid Hot

$T_H < T_{out}$

Figure 12. Control System Modes of Operation

While in operation, the 3-way control valve cycles on and off because of transport delays and temperature response lags in the plumbing and in the solar collectors. The control valve also cycles with a time varying duty cycle to accommodate variations in solar insolation and in inlet and outlet fluid temperatures.

The buffer tank functions to smooth out fluid temperature transients caused by the valve's switching as well as by temperature changes in the fluid returned from storage or from the heat engine. During system startup, the buffer tank also provides a reservoir of low temperature fluid which enables the solar collectors to come up to operating temperature without causing a subsequent high temperature overshoot.

A computer program was written to analyze the fluid control.[5] The analyses approach was to study the simplest system and if it did not work introduce minimal additional hardware. The first system analyzed did not have a buffer tank. The results are shown in Figure 13. This result was unsatisfactory as the heat transfer fluid was heated to temperatures too high for fluid chemical stability and temperature regulation was not adequate to maintain thermal storage thermocline stability. A buffer tank was then added and several iterations with different sizes of tanks were analyzed. Figure 14 shows the results operating with a 120 gal buffer tank. Satisfactory performance was achieved with is configuration. The results are shown for various insolation conditions in Figure 15. We believe the control developed is inexpensive, reliable and energy efficient for use in solar heat transfer fluid systems. The valve manufacturer has assured us that the valves will operate without leaking fluid. Since the hot heat transfer fluid has very low viscosity, tests of the valves have been designed and will be conducted before installing them in the field.

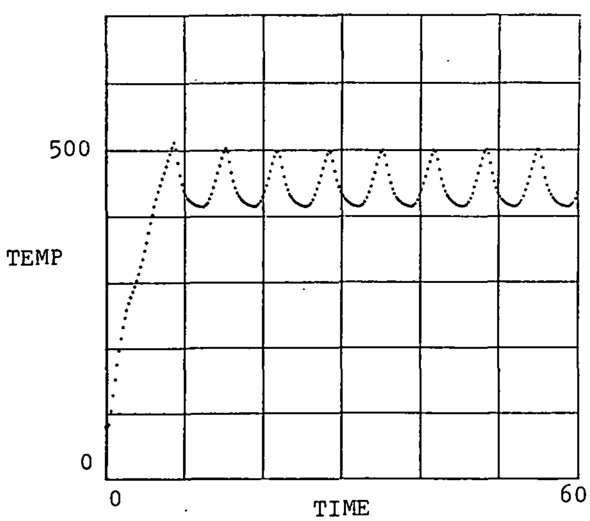


Figure 13. Flow Control Without Buffer Tank

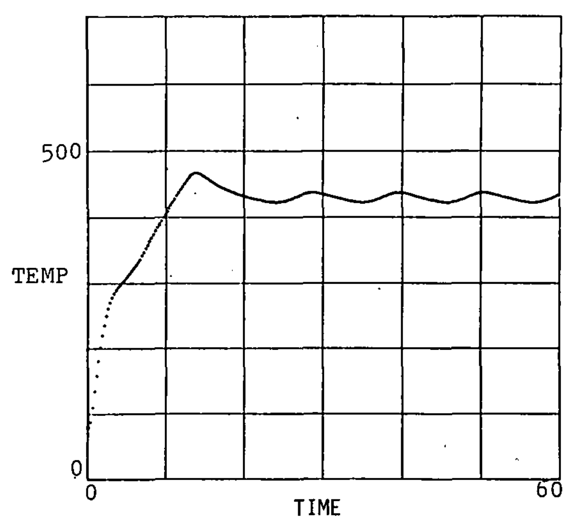


Figure 14. Flow Control With Buffer Tank

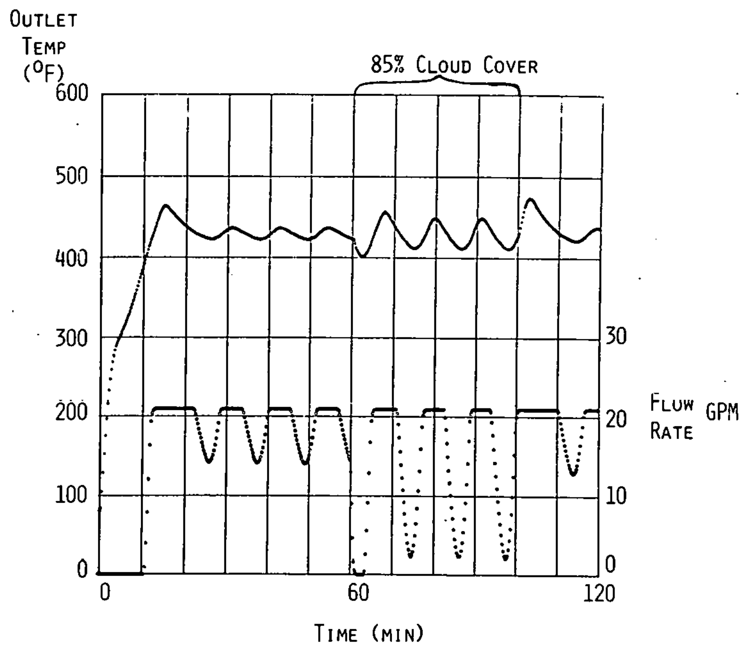


Figure 15. Response to Clouds--Computer Simulation Results

## Irrigation Well Characteristics

The owner of the experiment site, Ted Schrimsher, agreed to drill an irrigation well for this experiment. The well was drilled during December 1976, and was test pumped under the direction of Dr. George Abernathy, New Mexico State University.

The well drillers log (Table I) indicated the following information.

TABLE I

Well Drillers Log

| Depth (ft) | Formation | Depth (ft) | Formation |
|---|---|---|---|
| 0-8 | Sand | 120-135 | Sand and clay |
| 8-24 | Clay | 135-148 | Gravel and sand |
| 24-29 | Gravel | 148-153 | Clay |
| 29-47 | Sand and clay | 153-170 | Sand and gravel |
| 47-51 | Sand and gravel | 170-173 | Clay and sand |
| 51-86 | Clay | 173-187 | Gravel |
| 86-91 | Gravel, sand and water | 187-196 | Clay |
| 91-120 | Clay | 196-200 | Granite |

The well was pumped under conventional procedures for cleaning a new well. After the well had been cleaned, it was then pump tested to determine flow characteristics. The results are shown in Figure 16. From these results it was recognized that the water lift would be greater than previously estimated or the well was not as good as adjacent ones. A test of an adjacent well indicated the wells were equivalent.

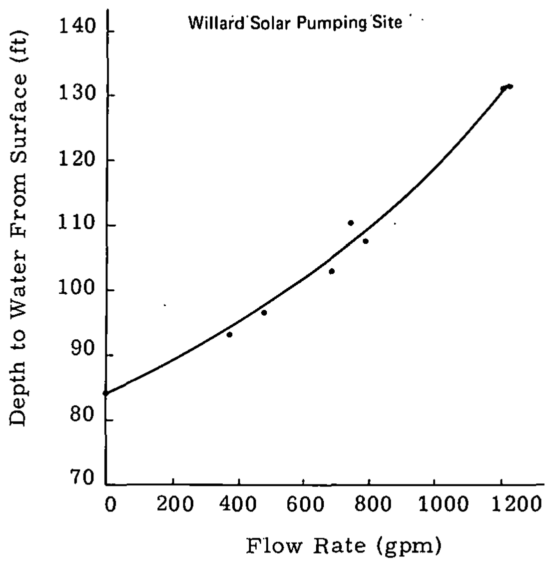


Figure 16. Well Flow Characteristics

With this well data and with data of commercial turbine pumps it was found that a pump could be purchased which would pump this well at 690 gpm, be within our power limits and operate at 84.5 percent efficiency. It will require five turbine stages to obtain this efficiency instead of the normal three. The expected five percent efficiency improvement over conventionally used pumps is not expected to exceed $2,000 more than other pumps and would be considered worth the extra cost. The pump purchase is part of the final phase of construction.

## Heat Engine Purchase

A heat engine was purchased utilizing the Request for Purchase as contained in Reference 1. Six different companies formally bid on the engine and two companies also bid on the low temperature engine. The bids ranged from $19,000 to $400,000. The medium temperature design (450°F) engine bids were lower than the low temperature ones (200°F).

The Request for Purchase stated that the proposals would be evaluated in conjunction with the collectors and the thermal storage to determine which heat engine would yield the highest performance. The evaluation was based on the following performance calculations:

$$\text{Performance} = \frac{(\text{Cost of Collectors})\left(\frac{\eta_t}{\eta_e}\right) + (\text{Cost of Thermal Storage})\left(\frac{\eta_t}{\eta_e}\right)\left(\frac{\Delta T}{\Delta T_1}\right) + \text{Cost of Engine}}{(\text{Power Output})\ (24\ \text{hr})}$$

$\eta_t$ is a theoretical efficiency based upon the desired engine output and the collector field performance.

It is written:

$$\eta_t = \frac{\text{Engine Output/Day}}{\text{Collector Energy/Day in June}}$$

$$\eta_t = \frac{(25\ \text{hp})(746\ \text{kW/hp})(3413\ \text{BTU/kW hr})(24\ \text{hr/Day})}{(1663\ \text{BTU/sq ft Day})(6720\ \text{sq ft})}$$

$$= \underline{\underline{0.137}}\ .$$

$\eta_e$ is a thermodynamic efficiency of the engine. It can be stated as:

$$\eta_e = \frac{\text{Engine Work--Parasitic Equipment}}{\text{Heat Transfer Fluid Energy Required}}\ .$$

Thermal storage was estimated to be 5000 gal with a usable temperature difference of 240 °F ($\Delta T$). The thermal storage cost was estimated to be \$3/gal including the fluid. $\Delta T_1$ is the temperature difference extracted from the fluid by the proposed engines. The larger the valve of $\Delta T_1$ the less thermal storage required. Also the engine efficiency effect the required collector field and thermal storage volume necessary. The cost of the collectors used in this calculation was \$97,440 for 6720 sq ft.

The performance results of the evaluation of the various bids ranged from \$306/hp hr to \$2508/hp hr. The medium temperature designs proposed has better performance than the low temperature ones. Barber-Nichols Engineering Company's bid resulted in the best performance and was purchased.[8]

The Barber-Nichols engine consisted of a boiler, turbine, gear box, regenerator, condenser and pumps necessary to produce 25 shaft horsepower at 1730 rpm. Its basic characteristics are:

| Type of Prime Mover | Price | Power | Heat Transfer Fluid | Performance |
|---|---|---|---|---|
| Turbine | \$74,171 | 25 hp | 420 °F Inlet<br>240 °F Outlet | \$306/hp hr or<br>\$213/hp hr at 100 ea |

A schematic of the engine is shown in Figure 17a and engine construction is shown in Figure 17b.

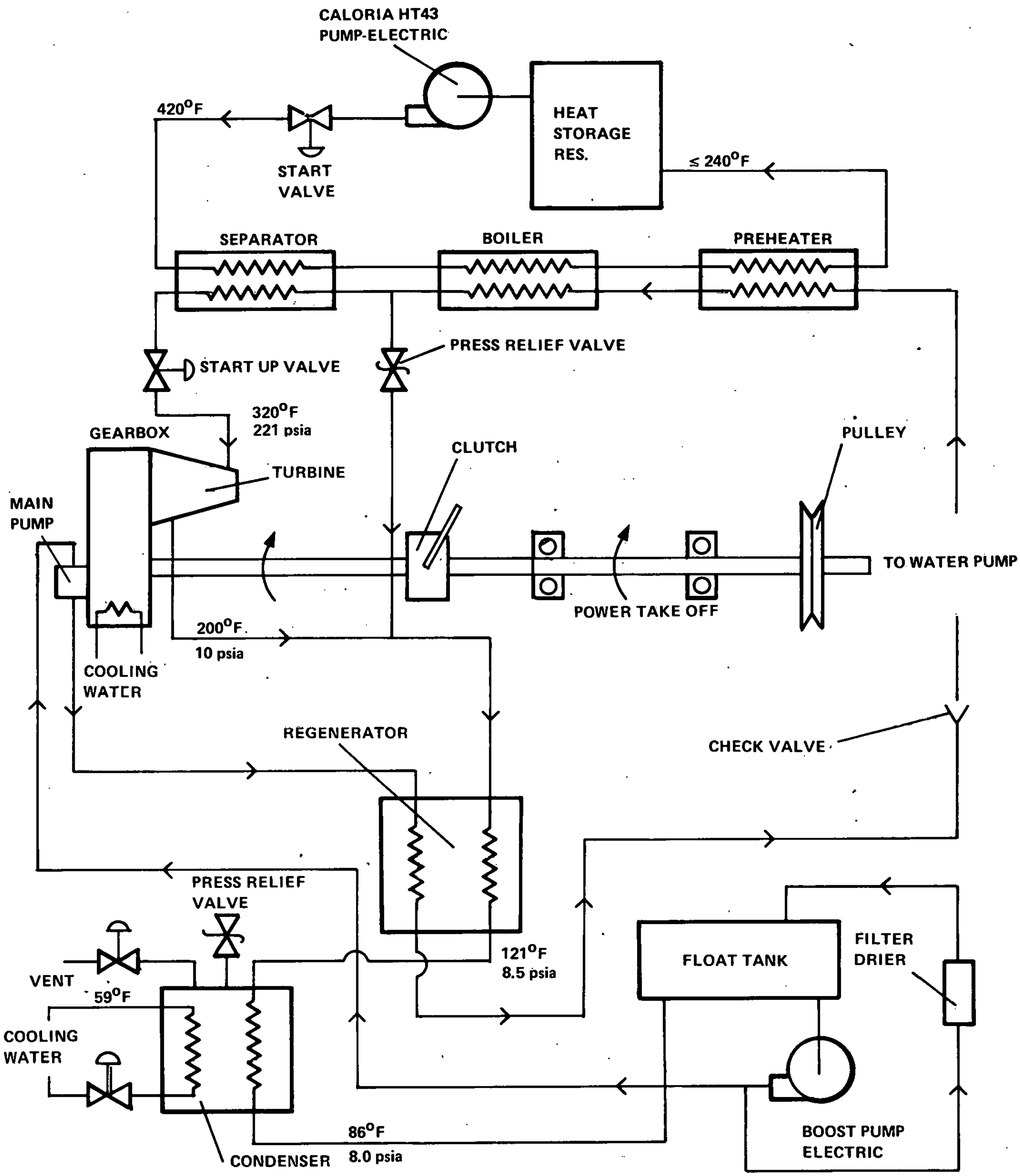


Figure 17a. Heat Engine Schematic

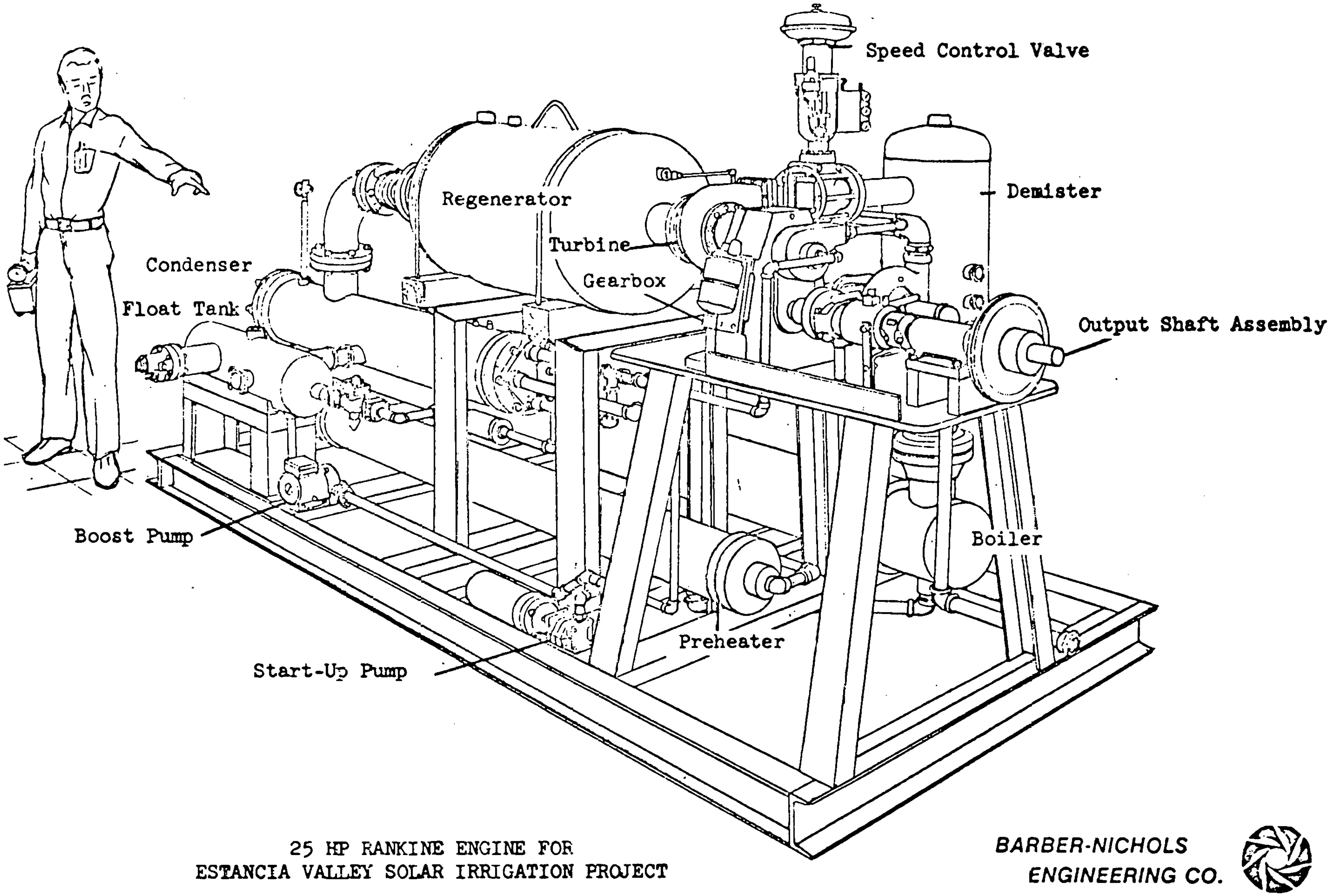


Figure 17b. Heat Engine Structure

Cost Effectiveness Study for Solar Thermal Energy Conversion System Utilizing Sensible Heat Source (J. Abbin)

The Request for Purchase for the heat engine for this experiment allowed suppliers to bid on either a low temperature (200°F) or a medium temperature (450°F) engine. Bids were received from several companies at varying operating temperatures. This information was then used to determine a performance versus cost as a function of operating temperature. The study is described below.

If we assume we have a system whose major cost items are the collectors, sensible heat thermal storage and a Rankine cycle engine; then the major system cost is given by:

$$\text{System Cost} = \text{Collector Cost} + \text{Thermal Storage Cost} + \text{Engine Cost.} \tag{a}$$

For the collectors a sufficient amount is needed to gather the desired energy, i.e.,

$$\text{Collector Cost} = \frac{K_1}{E} \tag{b}$$

where $K_1$ is the cost of collectors required to produce sufficient thermal energy at same baseline conversion efficiency and E is a variable conversion efficiency.

For a sensible heat thermal storage system the cost is given by

$$\text{Thermal Storage Cost} = \frac{K_2}{E\Delta T} \tag{o}$$

where $K_2$ is the cost of sufficient thermal storage to yield the required amount of energy with a baseline conversion efficiency (assembled to be the same as (b) above) and a baseline storage fluid $\Delta T$. E and $\Delta T$ in (c) are variable quantities which are related.

Figure 18 was obtained by plotting the cycle efficiencies and the associated $\Delta T$'s bid by the manufacturers who responded to RFP 05-0165 for the ERDA/New Mexico heat engine. The dotted line in Figure 18 gives a good fit for the top performing bids and agrees well with theoretical projections for a 420°F system. The function represented by the line in Figure 18 can fit nicely with a parabolic function of the form

$$\Delta T = K_3 + K_4E + K_5E^2 \text{ .} \tag{d}$$

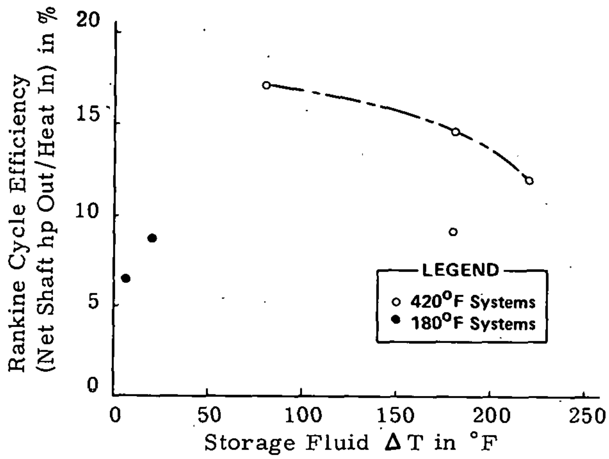


Figure 18. Quoted Cycle Efficiencies versus Storage Fluid ΔT

In general for the engine subsystem, the cost will be a weak function of the efficiency, but is a very stronger function of power level. Hence, for this analysis, the engine cost will be assumed to be a constant for the given power level, i.e.,

$$\text{Engine Cost} = K_6 \qquad \text{(e)}$$

by substituting b, c, d, and e into a we get

$$\text{System Cost} = \frac{K_1}{E} + \frac{K_2}{E\left[K_3 + K_4 E + K_5 E^2\right]} + K_6 \; . \qquad \text{(f)}$$

Thus we have system cost as a function of Rankine cycle engine efficiency only and we can determine what efficiency yields minimum system cost once we have determined the constants in equation (f).

In evaluating the engine quotes for the ERDA/New Mexico experiment, a baseline Rankine cycle energy conversion efficiency of 0.137 and a thermal storage ΔT of 240°F were used. The cost of the purchased collectors was $97,440, and these collectors are expected to collect 1.12 x $10^7$ BTU/day or 25 hp for 24 hours (600 hp hr) at the baseline conversion efficiency of 0.137. Thus, $K_1$ for the 25 hp system is

$$K_1 = \$97,440\ (0.137) = \$31,350 \qquad \text{(g)}$$

and we see in equation (f) that if the variable engine efficiency is greater than 0.137 then the total collector cost to produce 600 hp hr would be less than $97,440 and conversely if the engine efficiency were less than 0.137.

For the sensible heat storage, 5000 gallons of HT43 at $3/gallon including the cost of the tank and insulation were estimated to provide sufficient storage for 24-hour engine operation at a conversion efficiency of 0.137 and a ΔT of 240°F (again for a 25 hp engine output). Thus $K_2$ for this system is given by

$$K_2 = \frac{\$3}{\text{gal}}\ (5000\ \text{gal})\,(0.137)\,(240^\circ\text{F}) = \$493,200^\circ\text{F} \qquad \text{(h)}$$

and we see that in equation (c) if the variable engine efficiency E is greater than 0.137 and/or if the associated $\Delta T$ is greater than 240°F, then less than 5000 gallons of storage will be required and so on for various combinations of E and $\Delta T$. As stated earlier, however, cycle efficiency and $\Delta T$ are related. For this study the relationship was derived from the engine quotes and is shown in Figure 19. Fitting the curve in Figure 19, the following values for equation (d) were obtained:

$$K_3 = -549 \qquad K_4 = 12,800 \qquad K_5 = -53,400 \tag{i}$$

For the engine cost, $K_6$, a value of \$75,000 was used since this is the approximate award price of the contract for the 25 hp engine. Since the engine cost is not being considered as a variable, it will not affect the location of the minimum system cost point on the engine efficiency axis, but is included to yield major system cost.

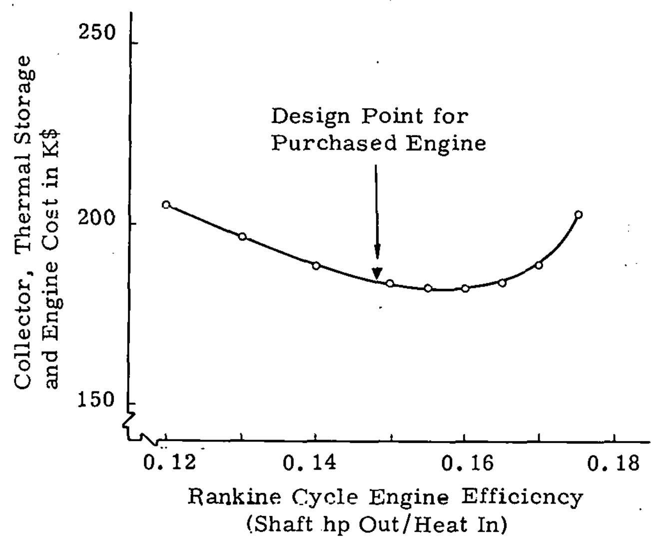


Figure 19. Major System Cost versus Engine Efficiency

Finally, the following cost equation for the 25 hp ERDA/New Mexico collector, thermal storage and engine system:

$$\text{System Cost} = \frac{\$13,350}{E} + \frac{\$493,200}{E[-549 + 12,800\,E - 53,400\,E^2]} + \$75,000 \; . \tag{j}$$

A plot of equation (j) is shown in Figure 19. We see that the minimum system cost occurs at an engine cycle efficiency of between 15% and 16%. Above these values the storage cost increases faster than the collector cost decreases and conversely below the minimum value. The projected cycle efficiency for the engine being purchased is 14.7%, which appears to be very close to optimum (within 3%) for the type of system chosen.

The same type of analysis as described above could be extended to different peak temperatures to produce a family of curves similar to Figure 19 for comparison and determination of the most economical system parameters.

## Pump Performance as a Function of Overpowering the Pump

It was suggested that thermal storage on the project might be deleted by allowing the engine and pump to be overpowered when the insolation was greater than the minimum amount required to drive the system. The result would be that of driving the system at a higher rpm than the design speed. This analysis was done to determine what results could be expected and how it compared to other options.

To do the analysis, it was assumed the engine and irrigation pump were of the turbine types. The system was sized to pump 500 gal/min when the insolation was 170 BTU/ft$^2$ hr and run at maximum efficiency. The pump ran at a design speed of 1875 rpm with a 5 ft head tolerance.

The pump characteristics were determined from the Hydraulic Handbook. The flow was given as being proportioned to rotating speed ($Q_1/Q_2 = N_1/N_2$), head was proportional to the squares of the speed $\left(H_1/H_2 = (N_1/N_2)^2\right)$, and the power was proportional to the cube of the speed $\left(P_1/P_2 = (N_1/N_2)^3\right)$. The efficiency of the engine turbine as a function of rotation speed was found in the Principle of Turbomachinery book by Sheppard and is shown in Figure 20.

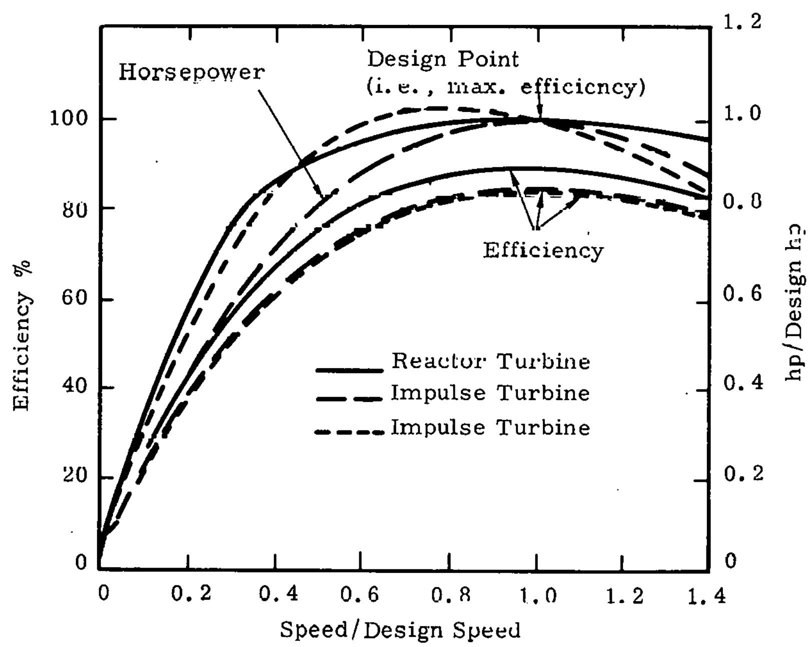


Figure 20. Performance Comparison of Turbines at Constant Pressure Ratio

With the above assumptions and reference data, the comparative performances were calculated. The ratio of pump, turbine and system change are those found when compared to a system operating at design speed. These are shown in Table II.

TABLE II

Pump Performance

| N(rpm) | Gal/min | Power hp | Ratio of Pump Performance | Ratio of Turbine Performance | % Change of Both |
|---|---|---|---|---|---|
| 1800 | 480 | 17.7 | 108.8 | 99.48 | + 8.2 |
| 1875 | 500 | 20.0 | 100.0 | 100.0 | 0 |
| 1900 | 507 | 20.8 | 97.5 | 99.85 | - 2.6 |
| 1950 | 520 | 22.5 | 92.5 | 99.56 | - 7.9 |
| 2000 | 533 | 24.3 | 87.5 | 99.26 | -30.8 |
| 2050 | 547 | 26.1 | 81.3 | 98.97 | -36.0 |
| 2100 | 560 | 28.1 | 80.0 | 98.44 | -38.2 |
| 2500 | 667 | 47.4 | 55.0 | 94.46 | -60.8 |
| 3000 | 800 | 81.9 | 38.8 | (no data) | 0 |

Utilizing this information along with the summer insolation for a 30° tilt flat plate collector as described in the Irrigation 189 form 7 (Ref. 1) the following was obtained (Table III).

TABLE III

Pumping Rate and Insolation

| Time of Day | Insolation ($BTU/ft^2$ hr) | Pumping Rate (gal/min) |
|---|---|---|
| 7 am | 100 | 0 |
| 8 | 175 | 500 |
| 9 | 240 | 565 |
| 10 | 290 | 580 |
| 11 | 320 | 589 |
| 12 | 325 | 594 |
| 1 pm | 320 | 589 |
| 2 | 290 | 580 |
| 3 | 240 | 565 |
| 4 | 175 | 500 |
| 5 | 100 | 0 |

This results in $2.737 \times 10^5$ gal/day of irrigation water being pumped. If all the insolation above 175 $BTU/ft^2$ hr were discarded, the amount pumped would have been $2.4 \times 10^5$ gal/day. If the energy above 175 $BTU/ft^2$ hr was stored and used at a later time, it would have pumped $3.57 \times 10^5$ gal/day. In other words, direct powering the system would increase the summer performance by 12.3 percent over that of rejecting all the insolation above 175 $BTU/ft^2$ hr. If the extra energy was stored and later used, the increase would be 48.9 percent over that of rejecting the extra energy. This comparison is graphically shown in Figure 21.

The indication is that on an energy basis thermal storage is worth approximately one-half of the collector cost. If, however, thermal efficiency can also be influenced by storage; then the difference in engine efficiency coupled with the calculated efficiency changes represent approximately an order of magnitude improvement in favor of storage.

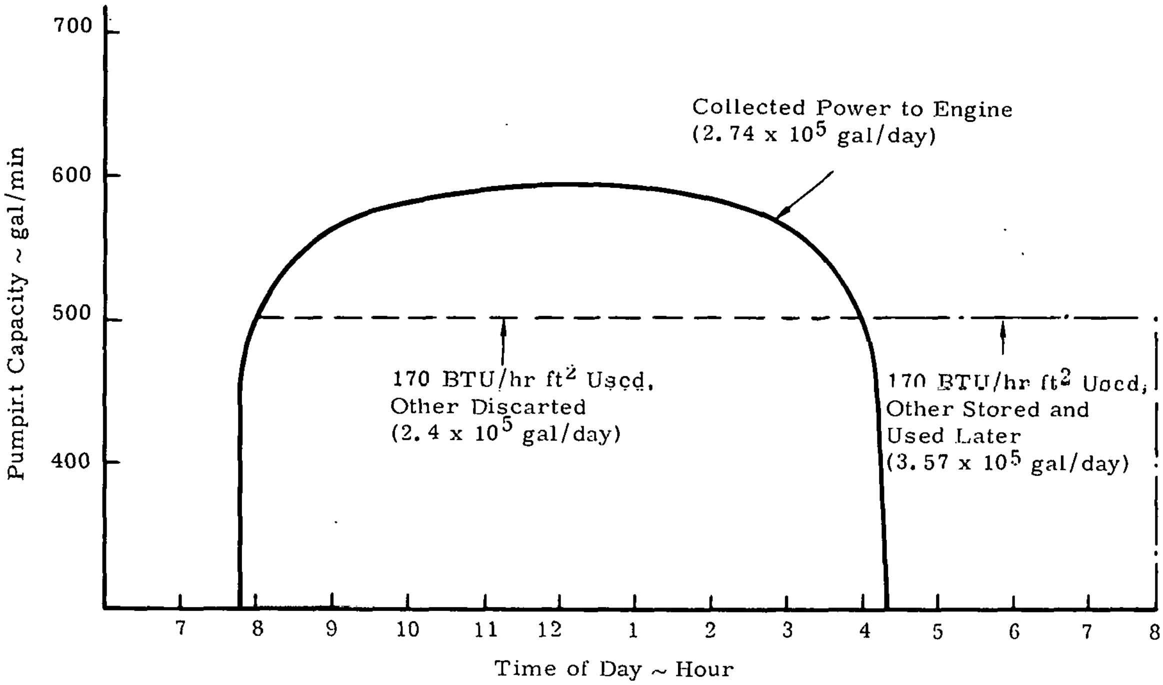


Figure 21. Pumping Capacity versus Time of Day

## Solar Collector Characteristics

Collectors for the experiment were purchased by New Mexico State University to the specifications listed in the Request for Purchase shown in Reference 1. Acurex Corporation was selected to be the supplier. Their design is a parabolic trough with a glass enclosed receiver tube located along the focal line. The units have an aperature of 6 ft and are 10 ft long. Eight of these are constructed together to form one large unit that is controlled by one motor and one tracking system. The collectors are a 90° rim angle design. The experiment utilizes 14 each of the 80 ft long units.

The receiver consists of a 1-1/4-inch diameter steel pipe that has an outer black chrome coating. A plug is contained inside the tube to reduce the volume of heat transfer fluid flow while maintaining turbulent flow. The plug allows a 0.1 in. annulus between the plug and pipe. The receiver tube is surrounded by a 2.0-inch O. D. x 1/8-inch wall Pyrex glass tube. The space between the glass tube and the receiver tube is at atmospheric pressure. Characteristics of the individual components are:

| | | | |
|---|---|---|---|
| Reflectance ($\rho$) | = 0.8 | Absorbitivity ($\alpha$) | = 0.94 |
| Glass Transmission ($\tau$) | = 0.9 | Emissivity ($\epsilon$) | = 0.1 to 0.2 |

The product of $\rho$, $\tau$, and $\alpha$ has been measured and is equal to 0.68.

An efficiency for the design was calculated. However, before the supplier for the collector was selected a trip was taken to his plant and a performance test was witnessed. The test result witnessed was at one insolation value and 450 °F heat transfer fluid exit temperature and the performance was compatible with their stated efficiencies. Therefore, Acurex efficiency data are reported here and is shown in Figure 22.

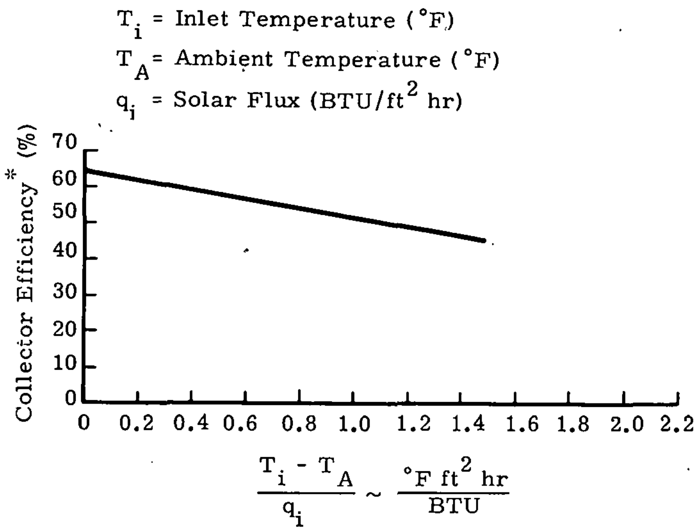


*Based on experimental data for a clear day, normal incidence, and no dust loss.

Figure 22. Collector Efficiency

Performance calculations were performed to determine the amount of energy that can be expected to be collected using these collectors at Albuquerque, New Mexico. Secondly, a question existed on which way the collector troughs should be oriented. Calculations performed by Jim Banas of Sandia Laboratories are shown in Figures 23 and 24. These figures indicate that during the summer months when irrigation water is necessary in New Mexico, that the collectors should be oriented in a north/south orientation. For an 8-month period the results are:

| East/West | | North/South | |
|---|---|---|---|
| Month | Energy Collected at 450 °F (BTU/sq ft Day) | Month | Energy Collected at 450 °F (BTU/sq ft Day |
| March | 1140 | March | 1420 |
| April | 1160 | April | 1710 |
| May | 1220 | May | 1885 |
| June | 1240 | June | 1900 |
| July | 1190 | July | 1840 |
| August | 1140 | August | 1740 |
| September | 1150 | September | 1560 |
| October | 1170 | October | 1250 |
| | 1176 | | 1663 |

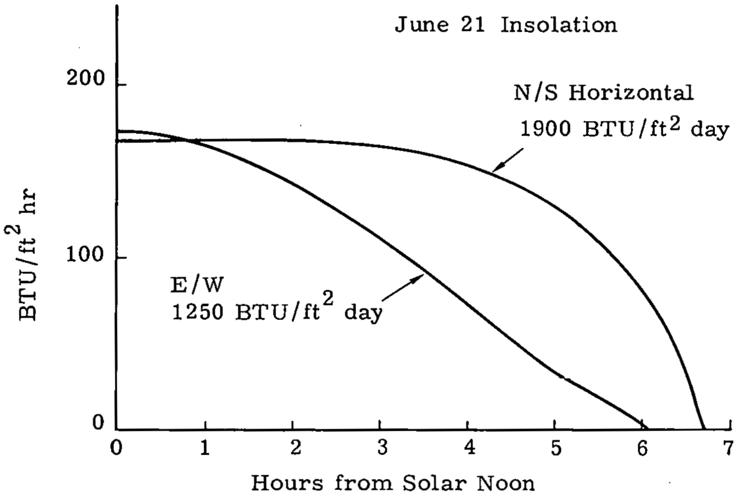


Figure 23. Collector Performance on Hourly Basis

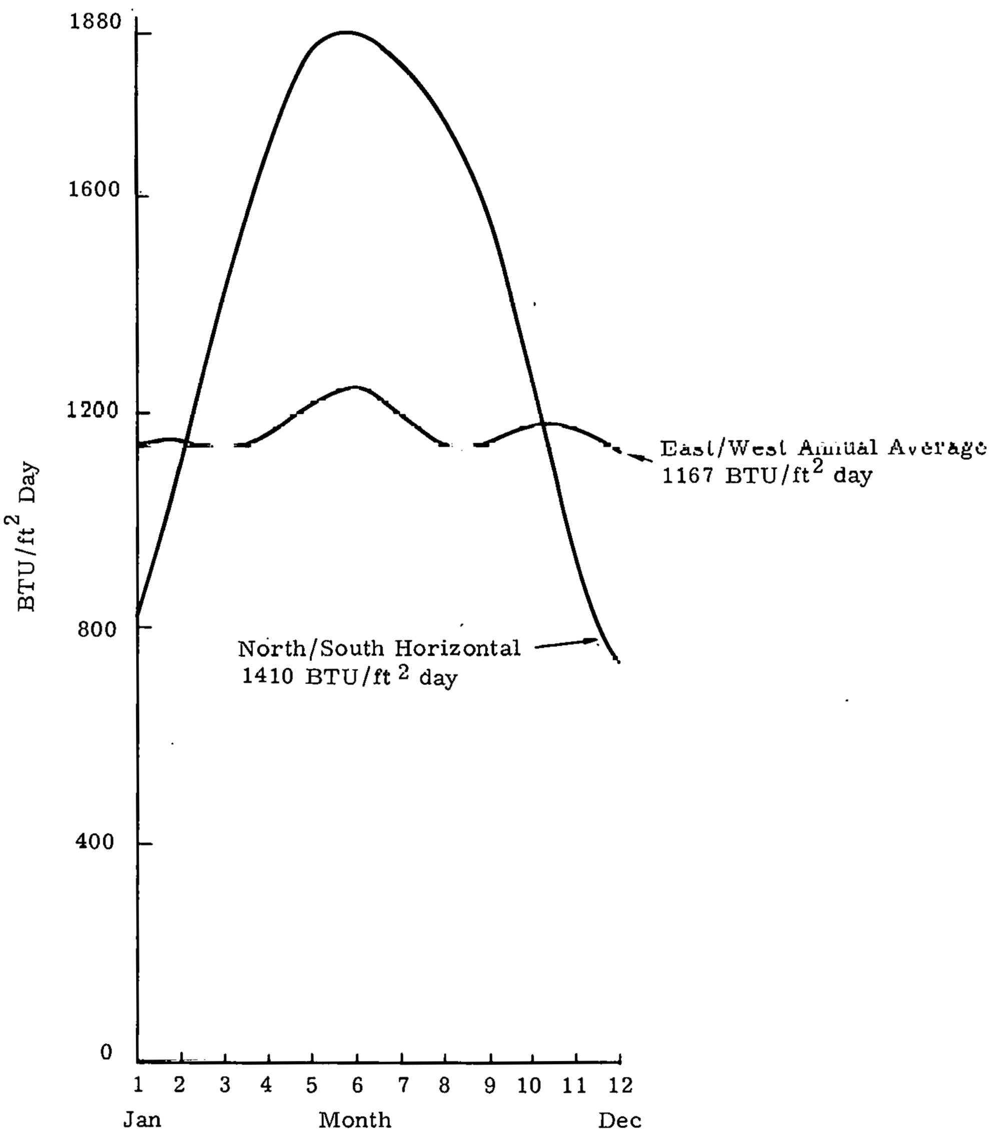


Figure 24. Collector Performance on Daily Basis

For these selected months, which is the growing season for New Mexico, the north/south orientation of the collectors results in approximately 41 percent more energy being collected. For this reason, the ERDA/New Mexico experiment has the collectors in the north/south orientation.

The complexity of construction of these collectors is illustrated in Figure 25. It should be recognized that the manufacture is simple compared to the automobile, tractor or airplane. This results in manufacturing cost per pound comparing favorable with the mass produced products at this time. This gives encouragement that the manufacturer's goal can be readily obtained. The energy collected in Albuquerque per year per sq ft of aperature in natural gas equivalent is shown for information purposes.

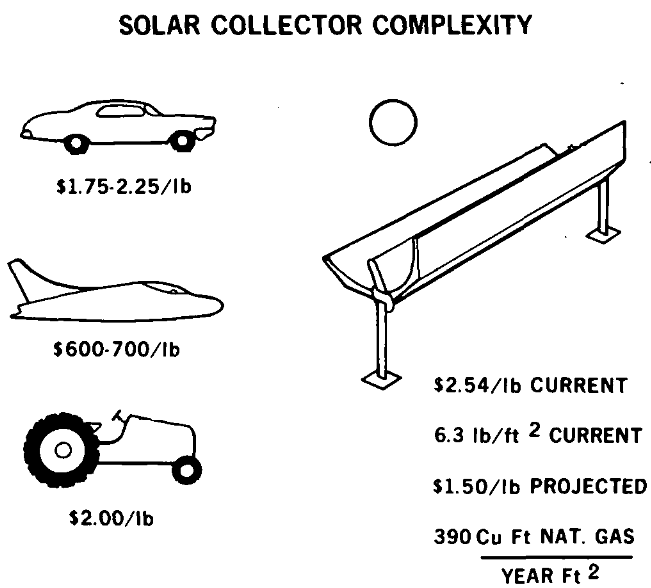


Figure 25. Collector Complexity Comparison

Hail Resistance Considerations (D. Miller)

Hailstorm data was assembled for Albuquerque, New Mexico, and surrounding area. The data indicated that Albuquerque could expect hail of 1/2 inch diameter or less up to seven times a year and over 1/2 inch diameter once in five years. Most of the hail storms were found to occur during the month of May. May, incidentally, is a month a solar irrigation system would be in use.

Hailstones have a mean density of approximately 0.8 gm/cm$^3$. Small hailstones, 0.078 to 0.157 inch in diameter, have a fall speed of 5 to 8 ft/s; medium size hail, 0.394 to 0.787 inch in diameter, have a fall speed of 39.3 and 52.5 ft/s, respectively; and large hail, 0.787 inch or larger, may reach velocities of 164 ft/s. From this data it is observed that a simulated hailstorm with one-inch diameter hail and a covering density of 300 to 500 balls/ft$^2$ would appear adequate for modeling a major hailstorm in the Albuquerque area. The data are graphically illustrated in Figures 26 and 27.

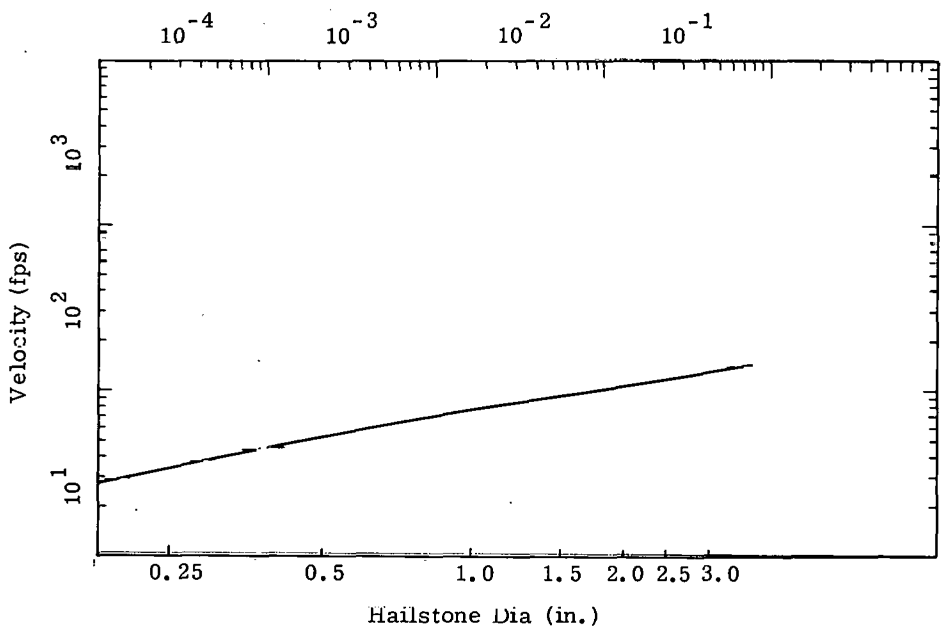


Figure 26. Theoretical Terminal Velocity of Hail

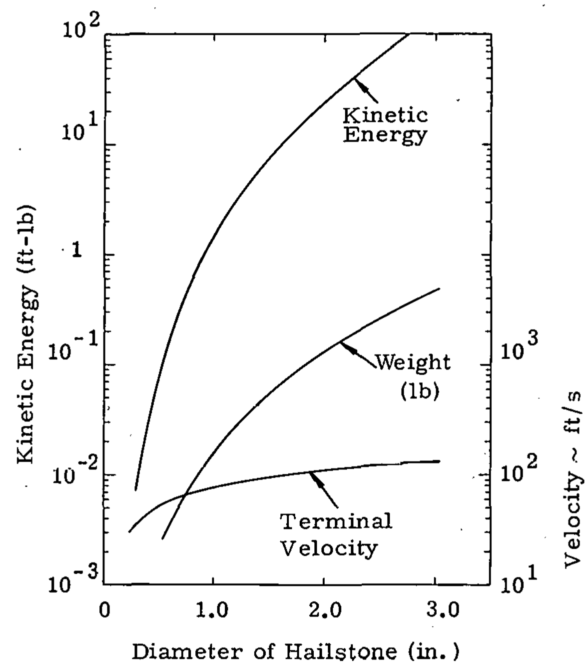


Figure 27. Diameter of Hailstones versus Kinetic Energy, Weight at Terminal Velocity.

After receiving the above hail information it was considered desirable if the collectors were hail resistant to 1/2-inch diameter hail. Tests were designed and conducted on potential reflective materials for collectors and the Alzak which was to be furnished on the collectors being purchased for the experiment. Alzak (0.025 inch thick) was tested with 1/2-inch diameter hail with the results being unacceptable damage. The dents were approximately 1/2 inch diameter and approximately 1/8 inch in depth. A test was devised in which a momentum trap material of less expense than the Alzak would receive the damage. A 2 ft x 2 ft plate of 0.025-inch thick Alzak resting on a sheet of 0.025-inch galvanized steel and supported by a frame only at the edges. The results are shown in Table IV. A typical dent profile recording is shown in Figure 28 and the majority of dents fit into two classes as shown in Figure 29.

TABLE IV

Hail Test Results

| Test | Ice Ball Dia. (in.) | Impact Velocity (ft/s) | Impact Angles (deg) | Dents/100 Balls | Dent Depth Mean (in.) | Dent Depth Std Dev (in.) | Dent Area Mean (in.$^2$) | Dent Area Std Dev (in.$^2$) |
|---|---|---|---|---|---|---|---|---|
| 1 | 0.75 | 45±2 | 90 | 91 | 0.0084 | 0.0033 | 0.339 | 0.139 |
| 2 | 0.75 | 45±2 | 45 | 88 | 0.0056 | 0.0032 | 0.242 | 0.099 |
| 3 | 0.5 | 45±6 | 90 | 68 | 0.0048 | 0.0017 | 0.196 | 0.099 |
| 4 | 0.5 | 45±6 | 45 | 67 | 0.003 | 0.0009 | 0.180 | 0.077 |

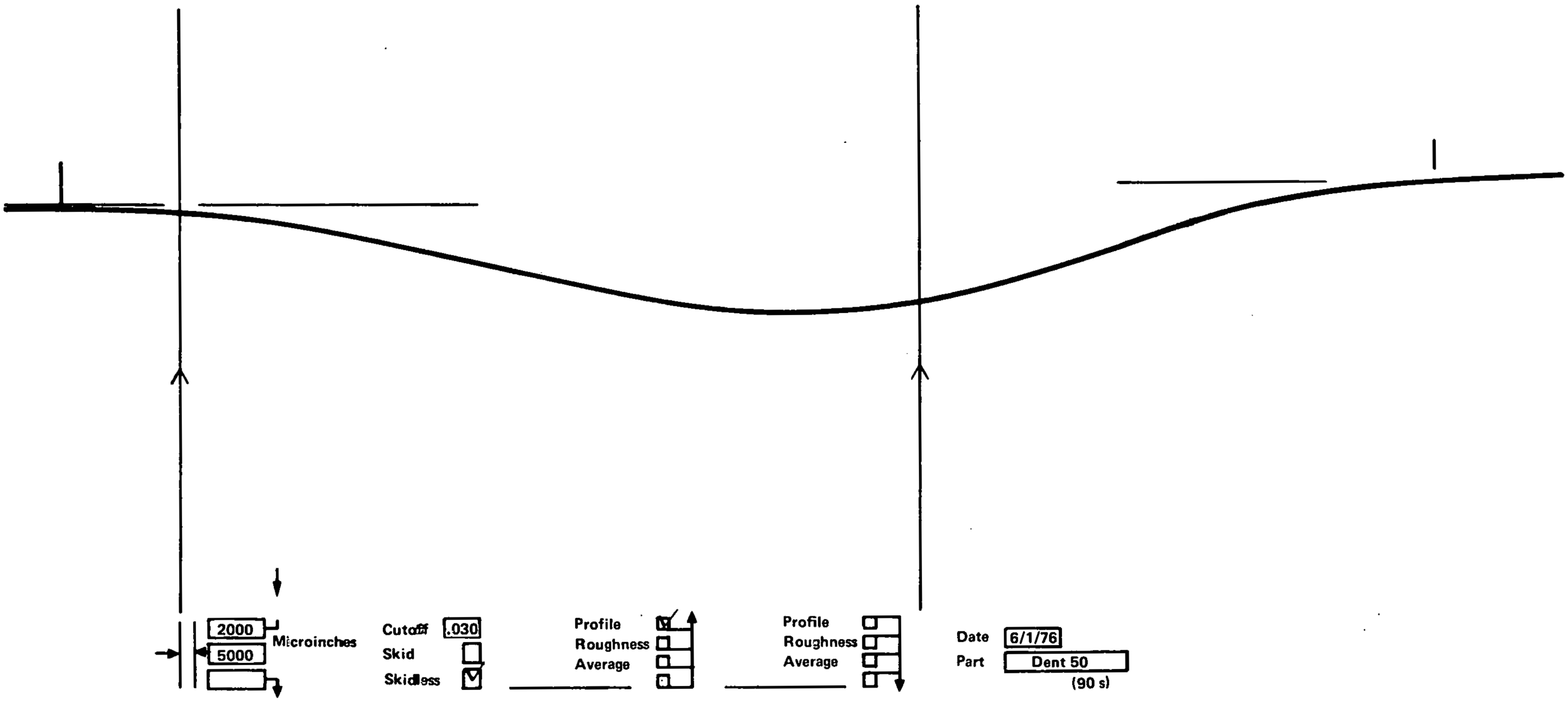


Figure 28. Typical Dent Profile

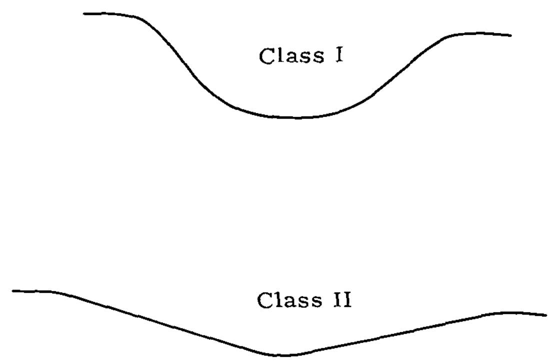


Figure 29. Dent Profile Class

Acurex Corporation was also working on the problem of hail damage. Their approach was to increase the thickness of Alzak until acceptable damage from 1/2-inch diameter hail was obtained. It was determined that 0.040 thick Alzak was sufficiently strong to limit damage. New Mexico State University agreed to purchase the thicker material for the ERDA/New Mexico collectors. A non-recurring cost of $5483 and a recurring material/cost of $6671 was paid for upgrading the collectors. A provision was also added to the system control to rotate the collectors upside down at the first detection of precipitation.

## Parabolic Collector Overheat (K. Wally)

One reason for the existence of an auxiliary power source is to allow the collectors to be stowed in the event of electrical supply failure so that the stalled collectors will not be subjected to an overheat situation which would lead to the degradation of the collector fluid or selective coating on the receiver tube. To evaluate the danger of an overheat situation, a transient thermal analysis was performed for several failure modes.

### Failure Mode 1

In this failure mode it is postulated that the system is operating properly when suddenly, all power to the system is lost. The collectors stop tracking the sun and collector fluid stops flowing. At this point, the collectors' components are at operating temperature. The sun continues to move with respect to the collector normal so that the solar flux decays. Figure 30a shows the transient solar flux per linear foot of receiver tube to which the receiver tube is subjected.

Figure 30b is a plot of the resultant receiver tube and collector fluid temperatures versus time. For this collector configuration and a solar flux of 325 BTU/hr $ft^2$, the maximum temperature attained by the receiver tube is just over 600°F. At this temperature and for the short duration of the transient, there is expected to be no significant degradation of the black-chromed selective surface. The maximum temperature attained by the collector fluid is approximately 575°F. This is below the 600°F which the manufacturer recommends as the maximum allowable bulk temperature for open system operation (i.e., fluid exposed to air at some point in the system). This analysis indicates that the collectors should survive an overheat situation resulting from a complete loss of system power.

### Failure Mode 2

In this failure mode, it is postulated that the collectors have been stowed in an orientation which allows the sun to pass through collector focus even if the system is not tracking. Such a situation would arise if a system power failure were to occur and were not corrected within 24 hours. It is assumed that the collectors are at the ambient temperature. As the sun moves with respect to the collector normal, the solar flux increases until the sun is in focus and then decays again as the sun passes out of focus. Figure 31a shows this transient solar flux per linear foot of receiver tube to which the receiver tube is subjected. Figure 31b is a plot of the resultant receiver tube and collector fluid temperatures. The maximum temperature attained is 500°F for the receiver tube and 475°F for the collector fluid. Both these temperatures are considered to be within the safe limits for these system components. This analysis indicates that the collectors should survive an overheat situation resulting from the transient collector heating due to the sun passing through the focus of a stationary, non-operating collector.

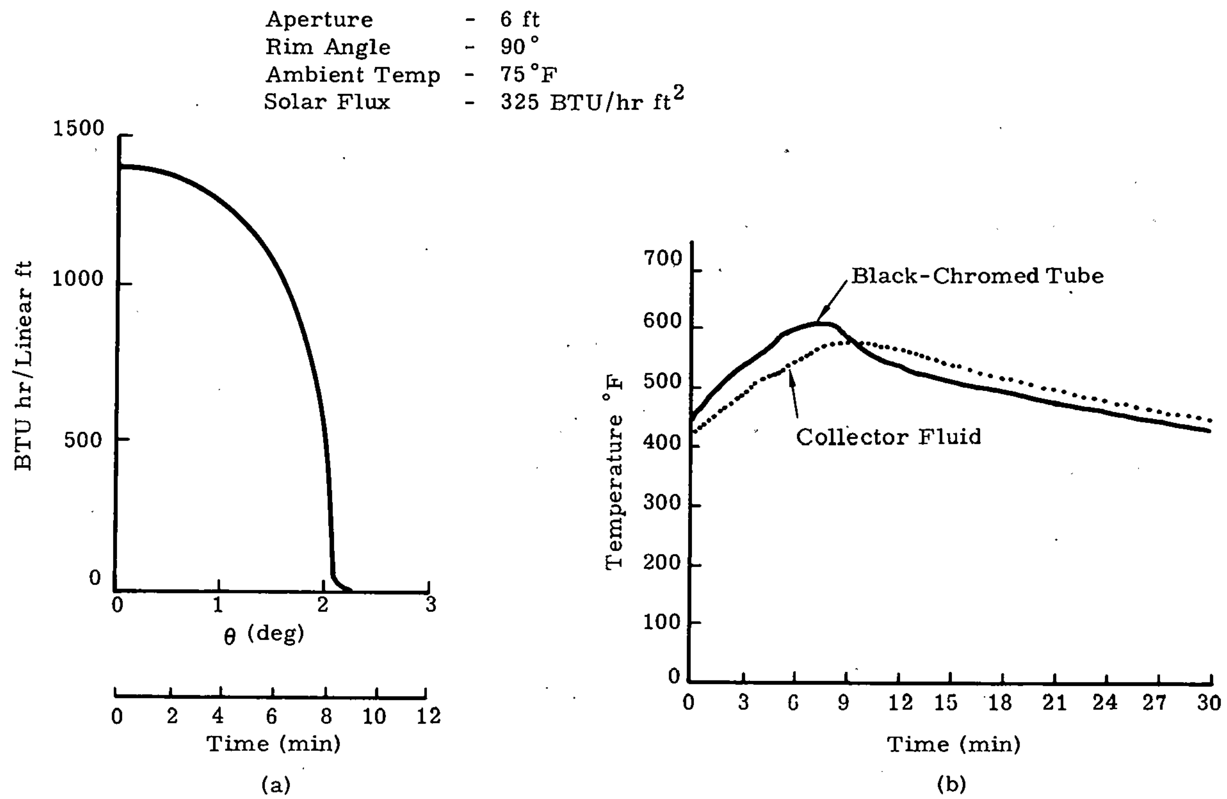


Figure 30. Transient Solar Flux per Linear Foot Receiver of Tube

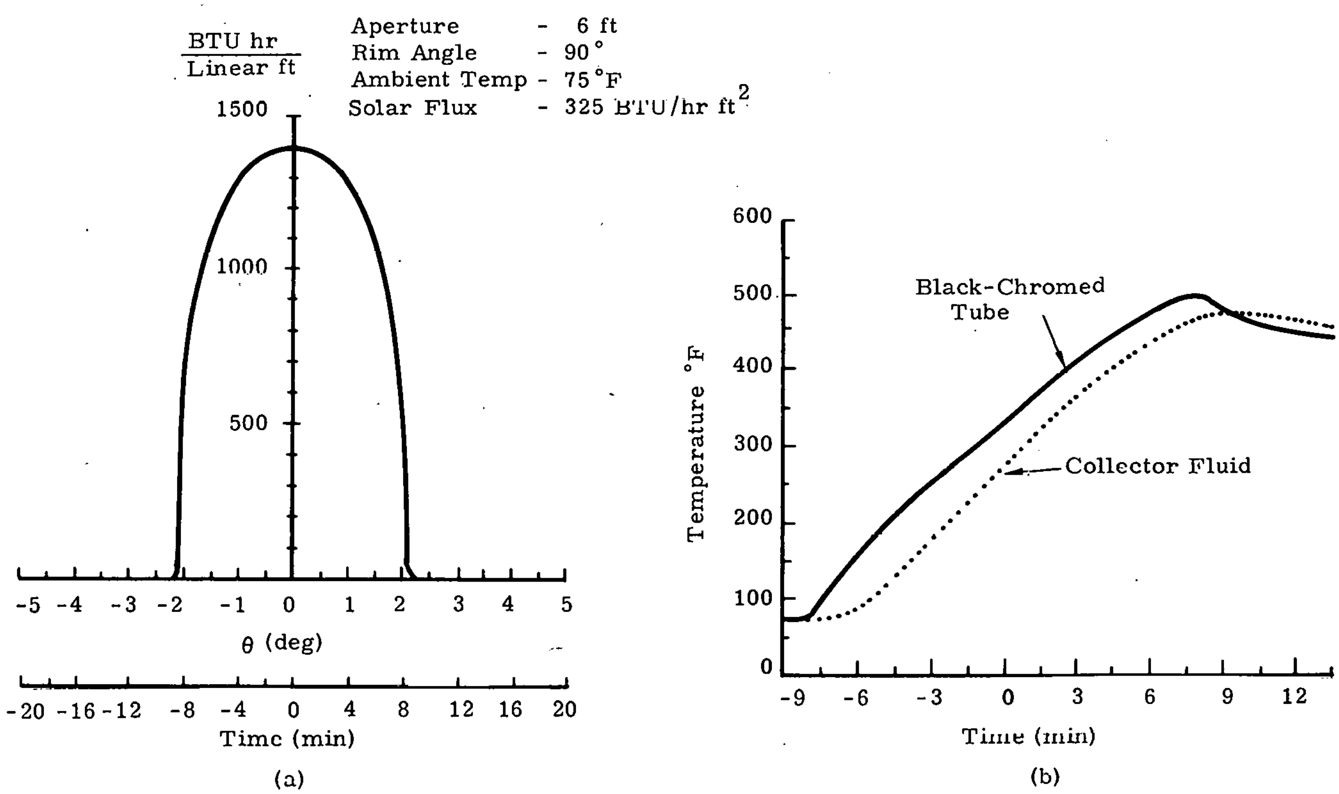


Figure 31. Transient Solar Flux per Linear Foot Receiver of Tube (not-tracking)

Failure Mode 3

In this failure mode, it is postulated that the collector fluid stops circulating (due to a pump motor failure, for example) while the collectors continue to track the sun. Continued tracking results in a constant solar flux (Figure 32a). The resultant receiver tube and collector fluid temperatures are plotted in Figure 32b versus time. In this failure mode, the component temperatures will continue to rise until equilibrium is attained. The process may be complicated by changes in component properties as a result of degradation due to elevated temperatures. The fluid failure temperature of 600 °F is attained in less than 9 minutes after system failure. This analysis indicates that the system will not survive this type of failure mode and, therefore, some type of safeguard is indicated. Monitoring of fluid operating temperature with collector detracking upon overheat appears feasible. The cross section of the receiver analyzed is shown in Figure 33.

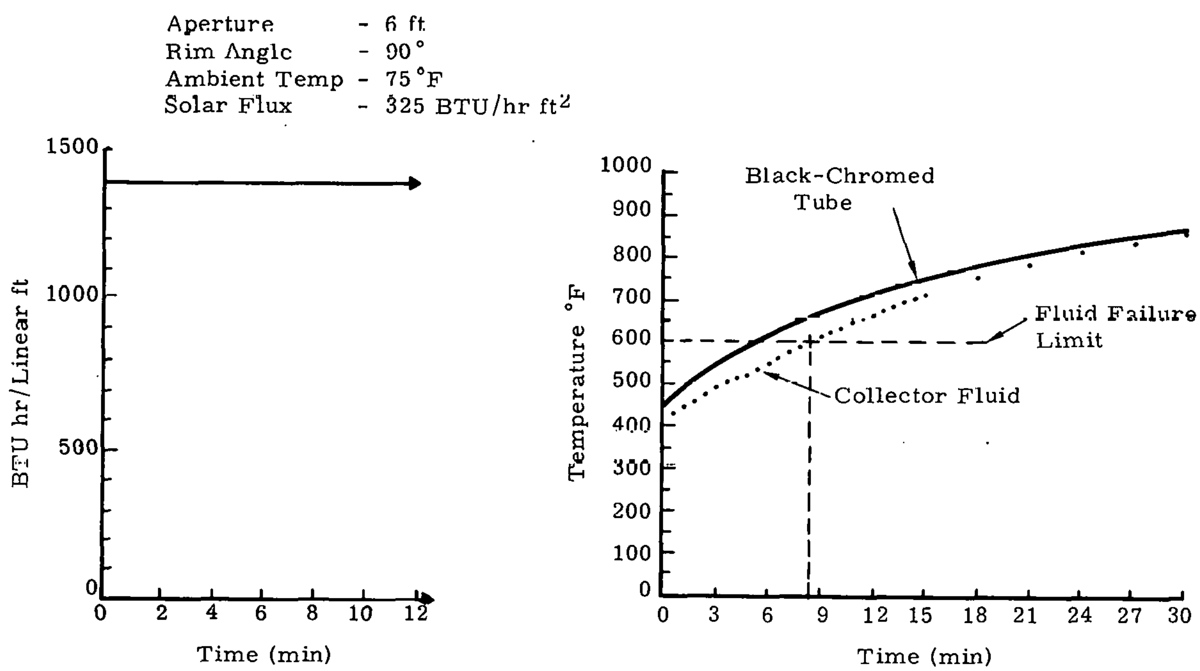


Figure 32. Receiver Temperature with no Fluid Flow

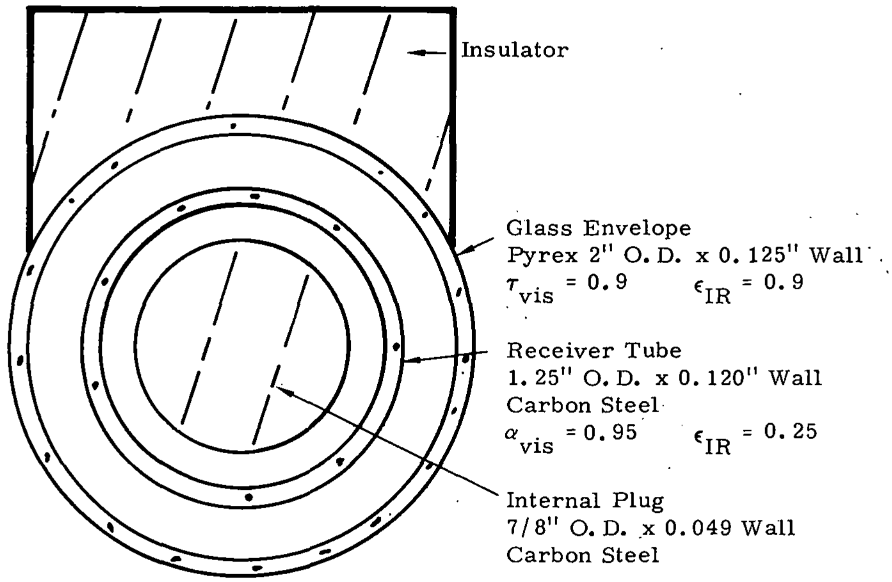


Figure 33. Receiver Cross Section

## Thermal Reservoir System

A low cost, reliable and personnel safe reservoir system has been designed. There are several design considerations for a thermal reservoir system utilizing flammable fluid and the thermocline technique. Some of these considerations are:

1) Hot fluid can only be added or withdrawn from the top of the reservoir
2) Cold fluid can only be added or withdrawn from the bottom of the reservoir
3) No air can be allowed in the reservoir which will oxidize the fluid
4) Fluid flow within the reservoir must be laminar to prevent the destruction of the thermocline
5) Reliable operation is required at minimum cost.

The reservoir system designed is illustrated in Figure 34. The reservoir size is 6500 gallons, the expansion tank is 8000 gallons, and the heat transfer fluid is Exxon Caloria HT43. The fluid will be received and stored in the expansion tank until the system is ready for operation. At this time the fill pump will be energized and cold fluid will enter the bottom of the reservoir through a diffuser. The air in the reservoir that is replaced by the fluid will be forced out the snorkel valve and the atmosphere via the expansion tank. When the fluid reaches the snorkel valve it will close and the fluid will then be forced up the standpipe until the highest switch of the three level indicator has been activated. This switch activation will de-energize the fill pump. As the fluid is removed from the bottom of the reservoir, heated by the collector field and returned, the fluid will expand. The required expansion (cold fluid) will overflow through the standpipe and return to the expansion tank. Therefore, the reservoir system is always vented to the atmosphere by either the snorkel valve or the standpipe overflow.

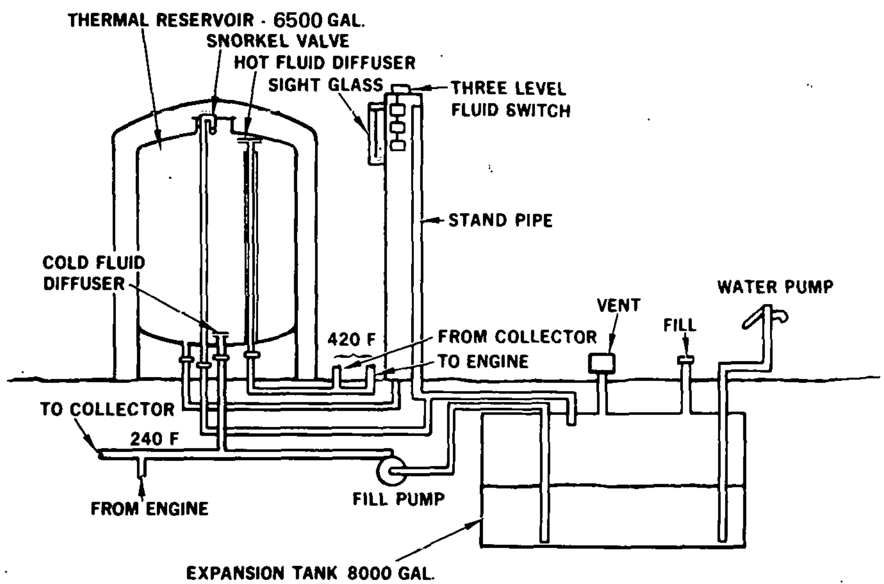


Figure 34. Thermal Reservoir System

When the system is in operation the reservoir may be gaining or losing in the amount of hot fluid it contains. Yet, to keep the fluid from oxidizing the reservoir must be kept full. This is accomplished by the tri-level fluid switch. After the top switch has been activated the pump is stopped and will turn on again when the fluid level has dropped to the middle switch. The pump will then continue to pump until the top switch is again activated. This will require approximately 5 gallons of fluid to be pumped. If the fluid ever recedes to the lowest level of the fluid level switch, the entire system is shut down due to lack of fluid or some other malfunction. The fluid in the standpipe is in contact with the air. However, this fluid is cool and the oxidation rate at this temperature is essentially zero.

Fluid flow in the reservoir is kept to a minimum by placing it in parallel with the collector field and the heat engine. The maximum flow from the collector field is 25 gpm and the maximum flow to the engine is 10 gpm. Therefore, the reservoir flow is 25 gpm to 10 gpm or 15 gpm since the heat engine will normally be running when maximum flow occurs. After sundown the heat engine alone will be operating, and it will withdraw its required 10 gpm. The engine is designed to operate until the maximum temperature in the reservoir reaches 350 °F. It is at approximately this temperature that the engine will be unable to power the pump. It is desirable that the reservoir be depleted of hot fluid each day so a narrow thermocline can be maintained.

The expansion tank is a conventional automobile service station tank. It is placed underground so that the earth can give it structural support, and so that the system can be drained by gravity into it in case of an emergency. The expansion tank is also slightly tilted so that any moisture condensate can accumulate at one end and be extracted by the pump.

The advantages of the design are:

- No nitrogen blanket is required on the heat transfer fluid.
- The reservoir operates at atmospheric pressure, has minimum flow which could disturb the thermocline, and can be drained for repair or in case of emergency.
- All pipes enter and exit from the bottom of the reservoir which facilities application of insulation.
- The standpipe and expansion tank requires no insulation.

## Simulation of Thermal Storage Reservoir Thermodynamics

A dynamic simulation of the thermal storage reservoir thermodynamics was performed to determine if the control system and storage reservoir volume which had been selected would provide the desired system operation. A computer program was developed in which the storage volume geometry is modeled as a cylinder of height, H; the two reservoir ends are modeled as oblate spheroidal volumes. For thermodynamic purposes the end volumes are treated as if the fluid contained in them is completely mixed, with resulting uniform thermophysical properties. The main reservoir volume is divided into 99 cylindrical layers, each treated as a mixed volume (Figure 35).

The end volumes are considerably larger than the individual layers in the main volume, but the presence of diffusers within the end volumes would appear to justify their modeling as mixed volumes.

Heat transfer within the fluid is modeled to include conduction and forced convection. No provision is made for free convection within the fluid. Under normal operation, free convection should not be significant. Tank walls of thickness, $\delta W$, are included in the model. It is assumed that a uniform temperature exists across the wall thickness. Conduction in the reservoir walls is one-dimensional because axial symmetry insures no polar variation in heat transfer. Heat transfer between the storage fluid and the reservoir walls is determined using appropriate empirical formulas for the convective heat transfer coefficient. The thermophysical properties of the Caloria HT43 storage fluid and the 1010 carbon steel reservoir are calculated as linear functions of temperature. Heat loss to ambient is determined using an overall heat transfer coefficient which includes the thermal resistance of the storage reservoir insulation and a surface convection coefficient for a moderate wind.

Reservoir Volume ~ 6550 Gallons

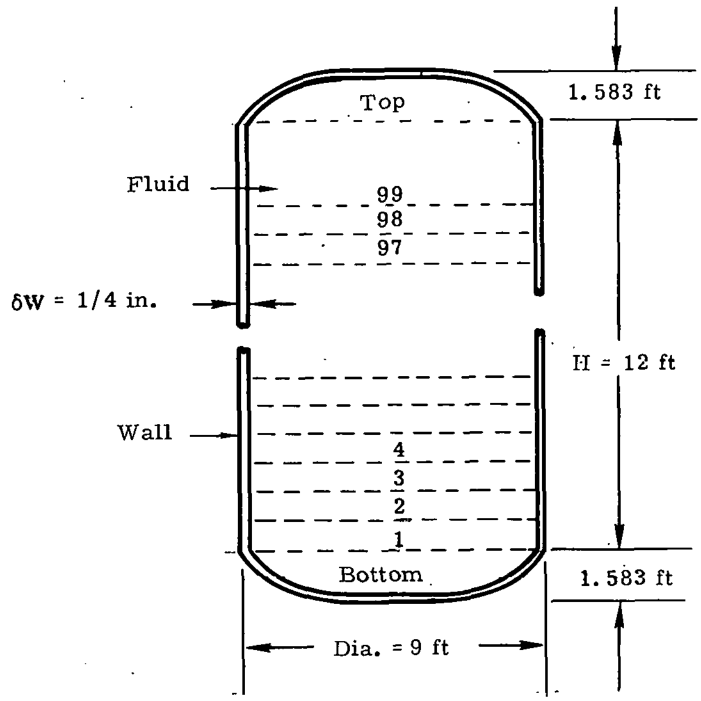


Figure 35. Thermal Reservoir Analyzed

There are four modes of thermal storage reservoir operation within the control system.

1) Full Charging - The entire collector flow rate $V_{COLL}$ delivers fluid at temperature $T_{HIGH}$ to the top node of the storage tank. This mode of operation is in force until the temperature at a specified tank level reaches a preset valve (approximately one hour). The resultant volume of hot fluid insures that once the heat engine is in operation, it will run continuously despite minor interruptions in solar flux due to clouds, etc. Adjusting the temperature and/or tank level of this control point allows the running time of the heat engine to be optimized.

2) Charging/Running - Part of the collector flow rate ($V_{COLL}$ - $V_{ENG}$) delivers fluid at temperature $T_{HIGH}$ to the top node. The remainder of the flow rate, $V_{ENG}$, goes to the heat engine. This is normal operation during daylight hours.

3) Discharging/Running - Fluid at temperature $T_{TOP}$ is drawn from the top node and is delivered to the heat engine at a flow rate $V_{ENG}$. Fluid at temperature $T_{LOW}$ is returned to the bottom node at a flow rate $V_{ENG}$. This is normal operation during nighttime hours.

4) Idle - There are no flows anywhere within the system. The only heat transfer is through conduction and loss to ambient. The mode of operation occurs when there is no collection of solar energy and the energy remaining in the storage tank is insufficient to operate the heat engine.

Results of several simulations are presented in Figures 36, 37, and 38 corresponding to summer, spring, and winter operation, respectively. These figures show the temperature profile in the tank as a function of time. Time zero corresponds to the time at which the system's photocells switch the system on.

The thermocline may be seen to move up and down the reservoir in a stable manner as the tank is discharged and charged.

During summer operation, 12 hours of charging (modes 1 and 2) completely fills the reservoir with hot fluid. This is sufficient storage to operate the heat engine for over 22 hours--very nearly continuous operation.

During winter operation, only six hours of charging is assumed. This is insufficient charging to completely fill the reservoir. As a result, there is only sufficient storage to operate the heat engine for slightly over 15 hours.

In addition to the results of Figures 36, 37, and 38, the simulations also indicated that the maximum differential between the wall temperature and the bulk fluid temperature would be approximately 8°C. This maximum differential occurs in the neighborhood of the thermocline when storage tank operation switches from charging to discharging. While this temperature difference is sufficient to produce significant free convection in the boundary layer along the reservoir wall, note that it occurs in the fluid levels which are most stable due to the density gradient in the neighborhood of the thermocline. Therefore, it does not appear that this free convection could significantly disturb the bulk of the fluid in the tank.

These simulations suggest that continuous 24-hour operation would be possible only under favorable summertime conditions. A larger storage volume could lengthen the operating duration of the system, but the economics of continuous operation versus storage costs are not sufficiently well defined to recommend such action. Note that during winter operation, the existing storage capacity cannot be completely charged and a larger capacity would be even more subject to this complaint. In order to more fully utilize the storage volume, it would be necessary to provide periodic operation in the full charging mode. This, in turn, would require deferment of heat engine operation during the full charging periods. Unavoidable storage inefficiencies make this an undesirable alternative from the point of view of system efficiency, although other considerations may indicate such operation.

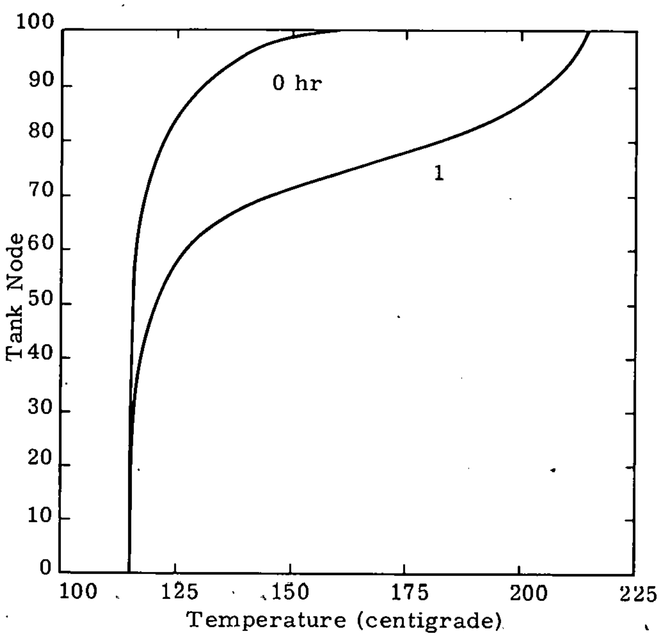


(a) Mode 1: Fully Charging Tank

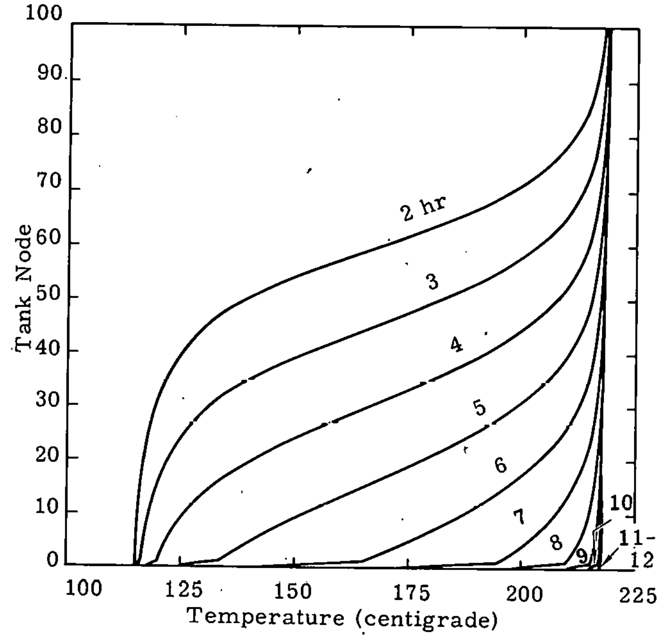


(b) Mode 2: Charging/Running Engine

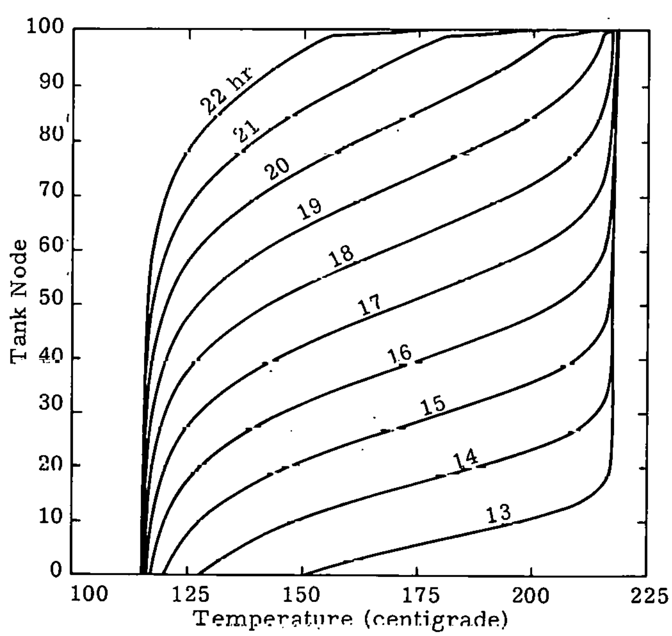


(c) Mode 3: Discharging/Running Engine

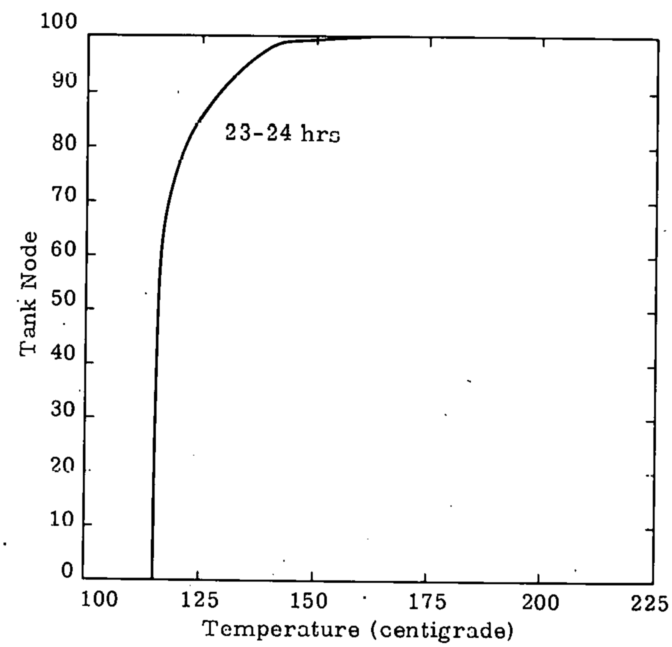


(d) Mode 4: System Off

Figure 36. Results of Thermal Storage Analysis (Summer - 12-hr Collection Day)

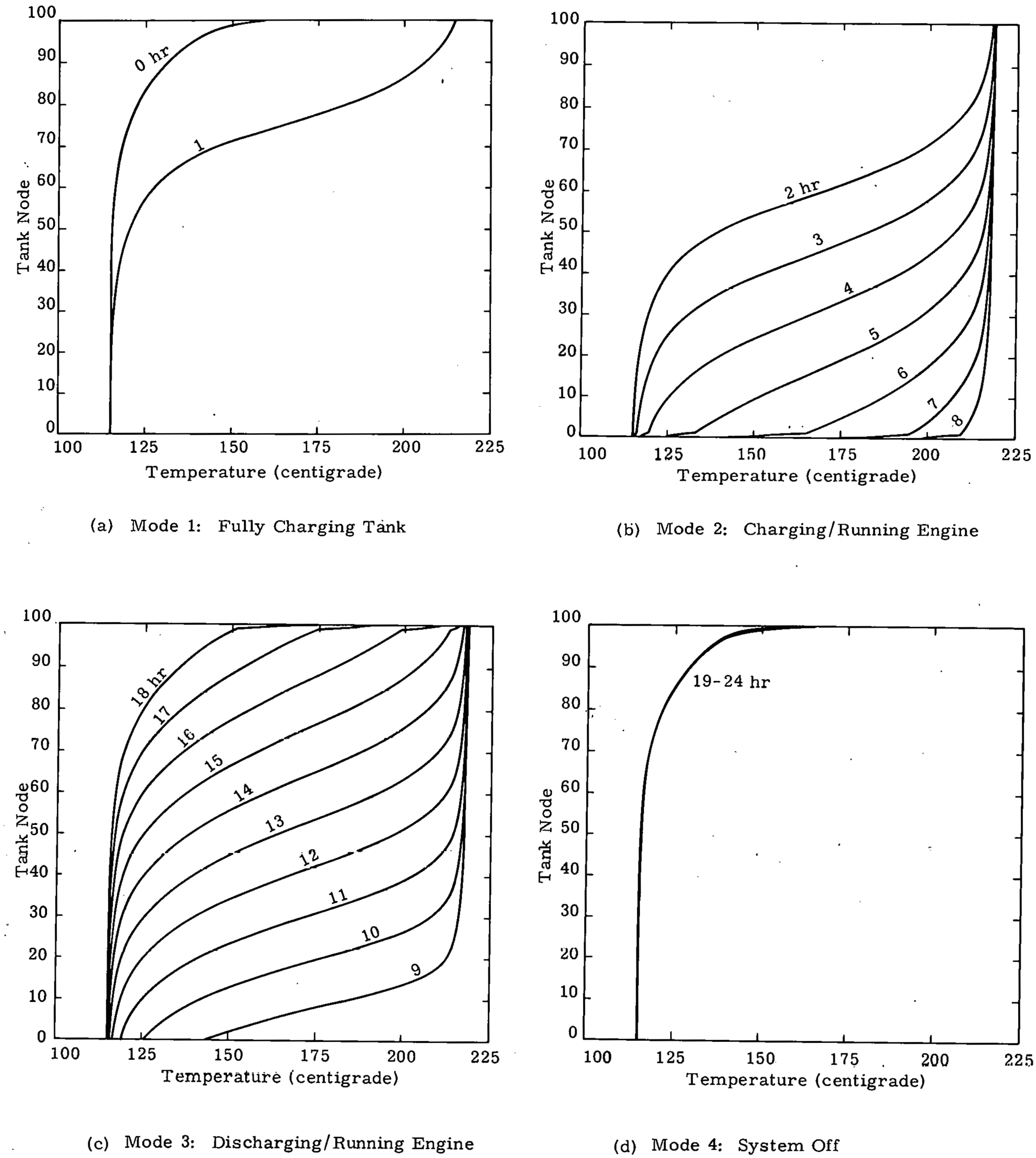


Figure 37. Results of Thermal Storage Analysis (Spring - 8-hr Collection Day)

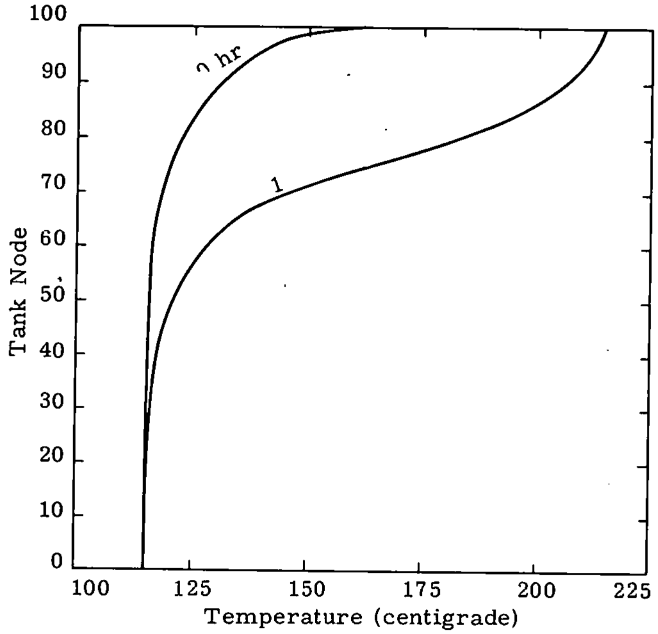


(a) Mode 1: Fully Charging Tank

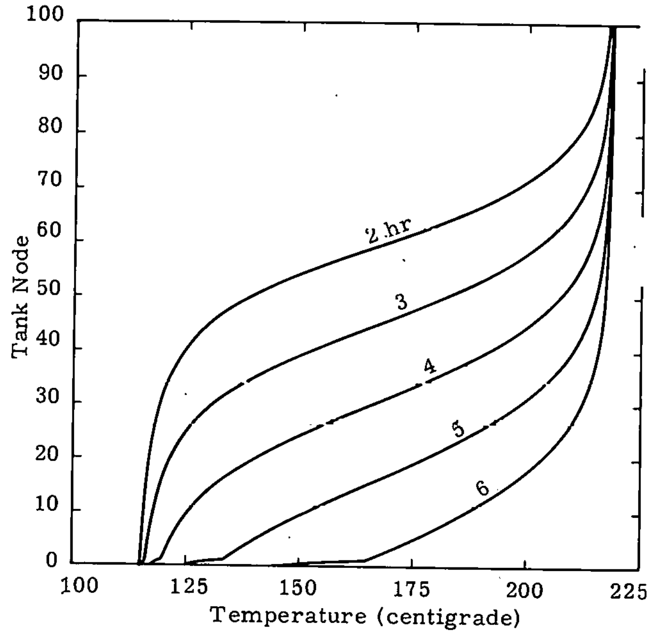


(b) Mode 2: Charging/Running Engine

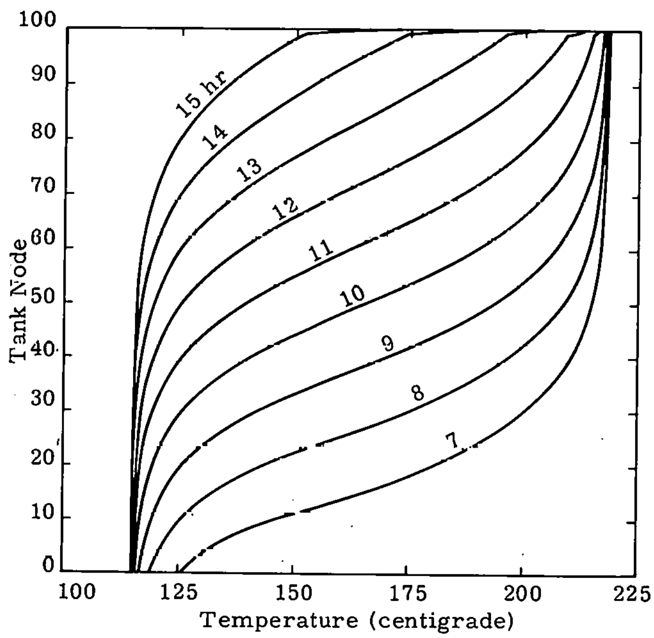


(c) Mode 3: Discharging/Running Engine

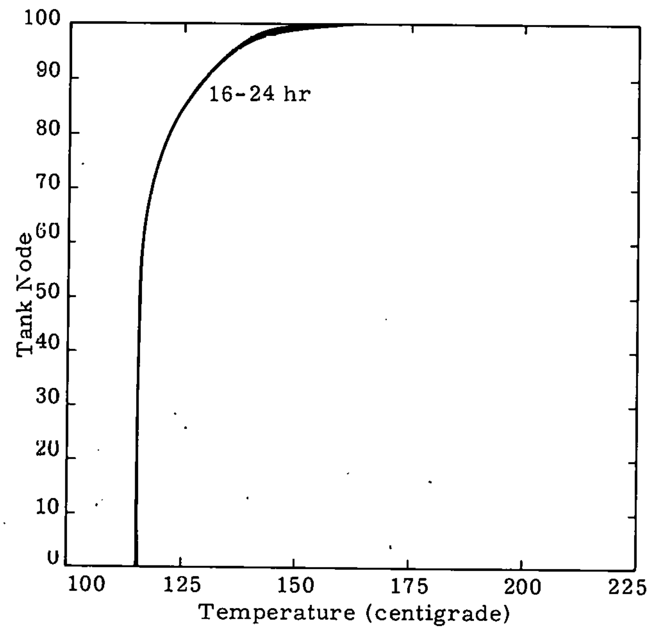


(d) Mode 4: System Off

Figure 38. Results of Thermal Storage Analysis (Winter - 6-hr Collection Day)

Consideration has also been given to the stability of a stratified thermal storage reservoir. This can be determined by the following:

The pressure at any arbitrating point in the fluid may be assumed to be $P_0$. Then for some small perturbation in the level of this fluid particle one has

$$P_1 = P_0 + \left.\frac{dP}{dh}\right|_0 dh \qquad \text{where } dh \text{ is the height moved.}$$

For fluids, the bulk modulus is essentially constant and is given by

$$K = \rho \frac{dP}{d\rho} \qquad \text{where } \rho \text{ is the density and } K \text{ is the bulk modulus.}$$

It follows that

$$\int_0^1 \frac{d\rho}{\rho} = \int_0^1 \frac{dP}{K}$$

$$\ln(\rho_1/\rho_0) = \frac{P_1 - P_0}{K} \qquad \text{or} \qquad \rho_1/\rho_0 = \exp\left(\frac{P_1 - P_0}{K}\right)$$

utilizing that $\exp(x) = 1 + X + \frac{X^2}{2!} + \ldots$

and $P_1 - P_0 = \left.\frac{dP}{dh}\right|_0 dh$ one obtains

$$\rho_1 \approx \rho_0 + \frac{\rho_0}{K} \left.\frac{dP}{dh}\right|_0 dh. \tag{A)}$$

However, $\rho_1$ is also given by

$$\rho_1 = \rho_0 + \left.\frac{d\rho}{dh}\right|_0 dh\,. \tag{B)}$$

Therefore, when A) $\geq$ B) the fluid is stable. When A) $<$ B) the fluid is unstable and will migrate to a new level due to its bouyancy.

The criteria for stability is therefore:

$$\frac{\rho_0}{K}\frac{dP}{dh}\bigg|_0 \geq \frac{d\rho}{dh}\bigg|_0 \quad \text{but} \quad \frac{dP}{dh}\bigg|_0 = -\rho_0 g$$

because of incompressibility of fluids; the criteria for stability becomes:

$$\frac{-\rho_0^2 g}{K} > \frac{d\rho}{dh}\bigg|_0$$

but $K >>> \rho_0^2 g$ and it reduces to $0 > \frac{d\rho}{dh}\Big|_0$ .

One should note that no "lapse rate" type of instability exits as in atmospheric meteorology due to incompressibility of the fluid.

## Control System Design Discussion

### Collector Control

The collector modes of operation are: track, de-steer, stow west or stow east. Under normal operating conditions the collectors will be stowed to the east. Stow position is an upside down position, but pointed slightly to the east or west. As the sun comes up in the morning, it is detected by a photocell whose operation energizes the collector fluid pump and the tracking system. A flow indicator switch must be activated by the fluid flow or the collectors will track only in the de-steer position. The de-steer position is only far enough away from track to prohibit the collectors from focusing on the receiver. The collector field will operate in the track condition if the fluid flows, the fluid exit temperature does not exceed 500°F, the reservoir is not full of hot fluid, the collector inlet temperature does not exceed 350°F, and precipitation is not occurring. When the sun goes down, the system will rotate back and stow to the east. All malfunctions will cause the collectors to de-steer. Precipitation or darkness cause them to stow. All of these functions have manual overrides.

### Heat Engine Control

The heat engine is commanded to run when a 110-volt electrical signal is supplied to the engine. The engine will run after receiving this signal if the collectors are operating and if a preselected amount of energy is stored in the thermal storage reservoir. If this condition is met, a globe valve between the engine and reservoir will open and the engine circulation pump will supply hot fluid to its boiler. The engine will continue to operate until either the pond is full or the reservoir depleted of 350°F or higher temperature fluid. It will both start and operate automatically unless manually commanded to do otherwise.

## Fluid Control

The fluid level switch in the standpipe controls the level of fluid in the reservoir. However, if the fluid level drops below the operating level, the entire system is shut down and will not operate until attended.

## Electrical Power

Some electrical power is used by the experiment. If utility power is interrupted for some reason, a standby power plant will automatically be activated and the experiment will continue to operate. When electrical service is restored, the backup supply will stop and the system will be switched back to utility power.

Wind versus Solar Power for Irrigation Pumping in the Estancia Valley (J. Alcone)

A preliminary analysis was conducted to determine the economic competitiveness of wind energy for pumping irrigation water in the Estancia Valley. Cost estimates of a vertical axis wind machine and the cost of the ERDA/New Mexico experiment were used along with their expected time of operation to determine the better performance.

The nearest known wind data for the Estancia area was that for Otto, New Mexico.[9] It indicated that approximately 25 percent of the time no wind power was available, 50 percent of the time 50 watt/$m^2$ was available, and 25 percent of the time over 700 watt/$m^2$ was available. From an inspection of the data it appeared that the wind blows approximately 75 percent of the time at an average power level of 270 watt/$m^2$ from February through October. The 270 watt/$m^2$ was used in the analysis.

The results indicated, based upon the 270 watt/$m^2$ wind energy, that a wind powered demonstration system would cost about the same as the ERDA/New Mexico experiment. Wind energy in the Estancia Valley does have one drawback that a similar system in another area may not have. This is that when irrigation is at its peak, June through August, the wind energy is at a minimum. This makes the storage cost for a wind system expensive and makes the wind energy approach not as practical as solar thermal.

Systems Analysis (Sharla Vandevender)

Regional/National Irrigation Requirements and Practices

The current effort in this task has been to develop a data base which will allow regional and national irrigation load characterizations. The data base must be assembled into a format usable for analysis. The initial data base will be for Arizona where one of the irrigation experiments will be located. The Arizona data base will be used as a model for development of the regional/ national data base.

The regionalization will be based on Water Resource Subareas (WRS), as defined by the Water Resources Council. These subareas approximate regions whose boundaries are delineated on the basis of topographic drainage characteristics. The subareas include groups of counties which, as closely as possible, approximate the actual drainage basin boundaries. The statistical data required for the irrigation data base is most frequently reported on a county basis, and by the Bureau of the Census on a Water Resource Subregion or Subarea basis. Grouping of WRS on the basis of agricultural characteristics and insolation characteristics will provide the regionalization criteria for the regional load characterization. This regionalization should reduce the total number of irrigation areas in the 17 western states which will be analyzed.

The data can be classified in several groups. These characterize the crops, wells, power sources for the irrigation systems and the water storage, and surface water pumping characteristics.

The well data required for each county follows:

- Number of irrigation wells by energy source
- Flow rate in gallons per minute (range, median, average)
- Lift (or water table depth plus drawdown) input (range, median, average)
- Water temperature in °C (range, median, average)
- Total annual operating hours (range, median, average)
- Distance between wells (range, median, average)
- Prime mover efficiency by energy source
- Annual energy consumption (BTU) by energy source
- Energy cost ($/million BTU) by energy source
- 1980 availability and cost of energy by energy source

The same data are required for surface water irrigation pumping as for wells (with obvious differences such as number of pumps).

The crop data required for each major crop in the county follows:

- Number of groundwater irrigated acres (range, median, average)
- Number of surfacewater irrigated acres (range, median, average)
- Irrigation system:

| | |
|---|---|
| flood<br>furrow<br>sprinkler | Total acres, acre-feet/acre and average efficiency per method. |

- Irrigated crop value per acre
- Irrigated yield per acre
- Inches of water applied per acre per half month

The water storage characteristics required include the efficiency of water storage (seepage loss), the evaporation rate and the cost of storage.

The availability of these data ranges from poor to good. Most of the required Arizona data are in hand, and it is currently being formatted. Inquiries are being made at the Bureau of the Census to ascertain the availability of county agricultural data currently reported in state summary form. Use of census data would provide for uniformity in the national characterization.

Economic Considerations (S. Vandevender and S. Varnado)

Inquiries are received almost on a daily basis regarding the economics of solar irrigation. Answers to these inquiries do not exist today as experiments are being conducted to determine the required information. These problems are, however, being addressed by Sandia Laboratories System Analysis Division directed by S. Varnado and by the Aerospace Corporation.

A preliminary economic analysis on solar irrigation has been attempted. Any results at this time are conjectural as little experimental data exists. The methodology selected was a discounted cash flow technique as defined by JPL for ERDA/EPRI. A complete description of the method can be found in the report: ERDA/JPL - 1012-76/3. This method is applicable to utility ownership of the solar system. A different methodology may be appropriate for farmer ownership. We are investigating this problem.

This methodology, as defined, calculates the busbar energy cost from a utility-owned solar electric system. The approach is also applicable to a privately owned system, provided the proper values for tax rate and discount rate are defined. Busbar costs represent the minimum price per unit of energy consistent with producing system-resultant revenues equal to the sum of system-resultant costs. This equality is expressed in present value terms, where the discount rate used reflects the rate of return required on invested capital. Major input variables include the output capabilities and capital cost of the energy system, the cash flow required for system operation and maintenance, and the financial structure and taxation level of the owner. This methodology has been programmed and used in the solar irrigation program. For comparison purposes, the evaluation has also been conducted on conventionally powered irrigation systems.

The solar system analyzed has not been optimized for size or mode of operation. One significant variable is the operating time of the system and another is the capital costs. The first analysis was done for an irrigation system retrofit where only the power source is replaced by a solar powered system. In this case the farmer is simply buying a new prime mover, powered either by solar, electricity, natural gas, or diesel fuel. All the costs are for the solar conversion. The second analysis is for a totally new irrigation system. That is, a new well, new pump, method of delivery, pump and engine. The analysis are shown below.

Solar Powered Retrofit System

Recent estimates have been obtained for a 25 hp system presently under construction in New Mexico. Estimates were for one of a kind and the 1000th unit. The results (Table V) were:

TABLE V

Estimated Component Cost

| | 1 Unit | 1000th Unit |
|---|---|---|
| Prime Mover | $ 78,000 | $ 7,000 |
| Collector (6720 $ft^2$) | 98,000 | 33,550 |
| Thermal Storage (6500 gal) | 19,500 | 12,000 |
| Accessories | 12,000 | 4,000 |
| Construction | 10,000 | 4,000 |
| | $217,500 | $60,550 |

The cost of natural gas to the New Mexico farmer is $1.40/mcf. They have been informed to expect the price to be $5.00/mcf by 1982. For this analysis the engine efficiency for burning natural gas was estimated to be 20 percent, cost $5,300 new, and last 8000 hours. This replacement cost is included in the economic evaluation.

For diesel fuel the same 20 percent efficiency was used. This translates into a diesel fuel consumption rate of 2.4 gal/hr. Two fuel costs were assumed: $0.55/gal and $1.00/gal.

An electrical system has the lowest capital cost if the power is available at site and the transformers are supplied by the utility company. A conversion efficiency of the motor was assumed to be 90 percent. At an efficiency of 90 percent, 21.5 kW of electricity are required to provide 25 shaft hp. The annual cost of this power is $776 at 2¢/kW hr and $3879 at 10¢/kW hr. The motor is estimated to cost $700.

New Solar Irrigation System

The cost of purchasing and installing a new irrigation system in the Estancia Valley of New Mexico is estimated to be $50,000. This includes a new well, pump and irrigation system. In order to investigate the effects on irrigation costs of these higher capital costs, the program was rerun with $50,000 added to the capital cost estimates for the retrofit application. An additional $5000 was added to the electrical system to simulate the extension of the power line for one mile. The capital cost estimates are given below and the fuel cost remained the same as before.

(a) Solar

1 unit - $267,500

1000 unit - $110,550

(b) Natural Gas

1st year - $55,300

17th year - $ 5,300
(engine replacement)

(c) Diesel

Same as (b)

(d) Electricity

$55,700

In addition to the capital and fuel cost estimates given above, an estimate of the operations and maintenance costs for each system is also needed. There is, as yet, no indication of what this cost would be for solar systems. For conventional systems, the annual operating and maintenance (O&M) costs are typically estimated as 5 percent of the capital costs for a plant operating year round.

Other economic parameters assumed (Table VI) are as follows:

TABLE VI

Economic Parameters for Study*

| | |
|---|---|
| Year of Commercial Operation | 1978 |
| Price Year | 1977 |
| Base Year | 1977 |
| Year of First Expenditure | 1977 |
| Tax Rate | 20.0% |
| Discount Rate | 8.5% |
| General Inflation Rate | 5.0% |
| Capital Inflation Rate | 5.0% |
| Operation and Maintenance Inflation Rate | 6.0% |
| Fuel Inflation Rate | 6.0% |
| System Lifetime | 20 Years |

*These numbers may not be representative but are the value used for this study.

These parameters were used as input to the discounted cash flow analysis in order to compute the levelized busbar energy cost for the different systems. The results are presented in Figures 39 through 41 for both the retrofit and Figures 42 and 43 for the new installation cases. The solid lines are for the solar system and the dashed lines are for the alternative energy listed.

It should be emphasized that these curves apply <u>only</u> to the Estancia Valley situation and its associated insolation.

The results for the retrofit case indicate that if the collectors cost near the $\$5/ft^2$ and natural gas cost $5 mcf, it would be economic to use solar if the system operated more than 2200 hr/year. At $1.40 mcf gas, the solar powered unit would not compete. For electricity, solar would compete with 10 ¢/kW-hr at approximately 1900 hr/year. Solar would compete with diesel at 55 ¢/gal at 2600 hr/year. In each case if the collectors cost $\$14.60/ft^2$, the conventional method would be the most economical choice.

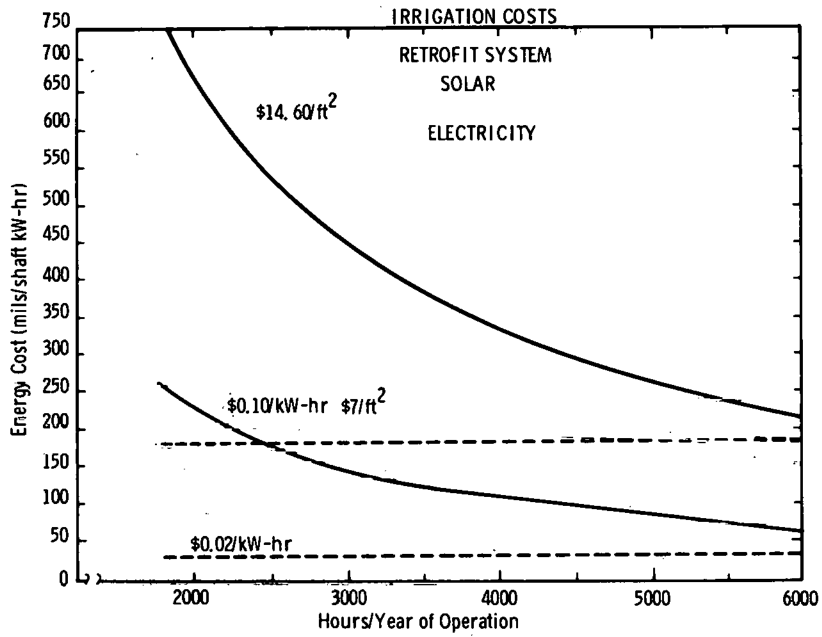


Figure 39. Economic Comparison of Solar versus Electricity for Retrofit Case

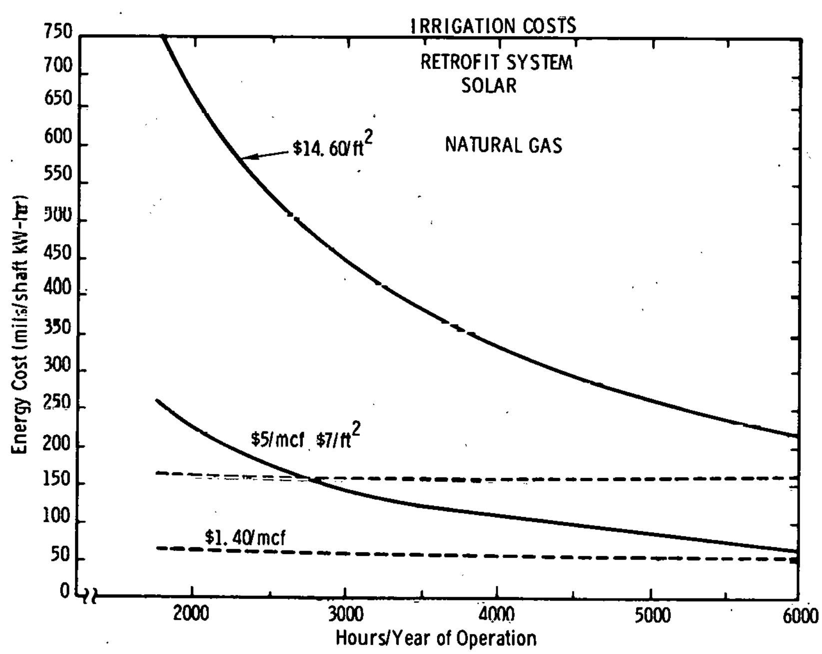


Figure 40. Economic Comparison of Solar versus Natural Gas for Retrofit Case

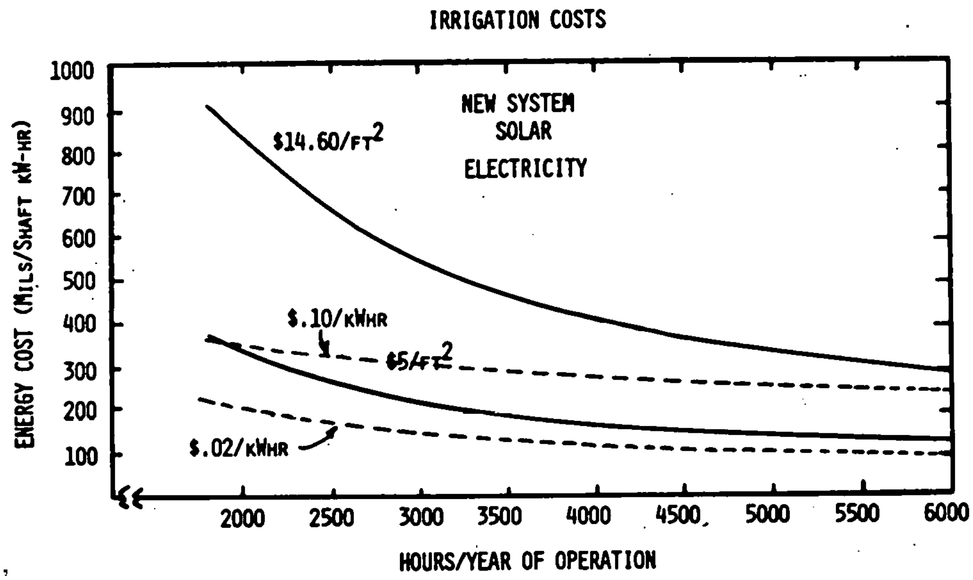


Figure 41. Economic Comparison of Solar versus Electricity for New System

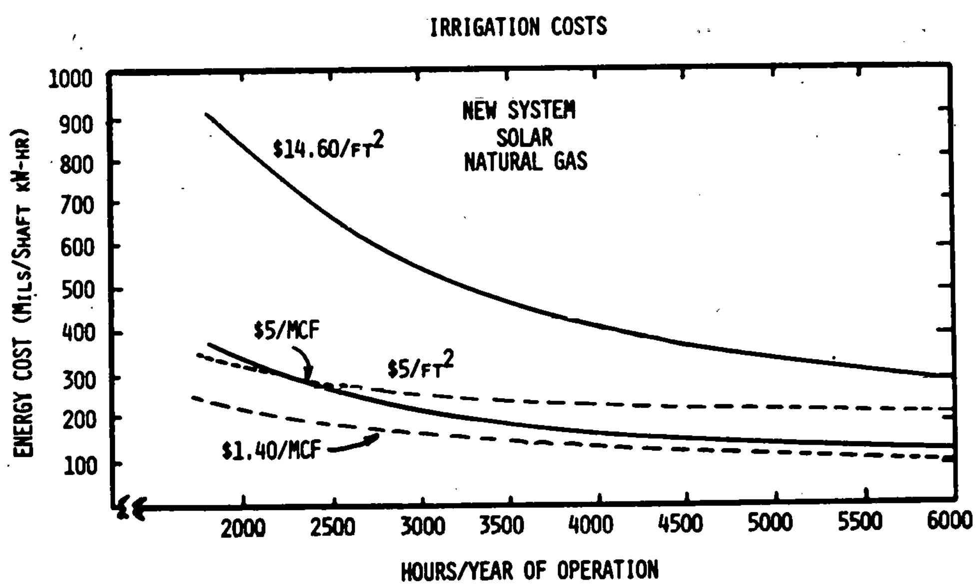


Figure 42. Economic Comparison of Solar Versus Natural Gas for New System

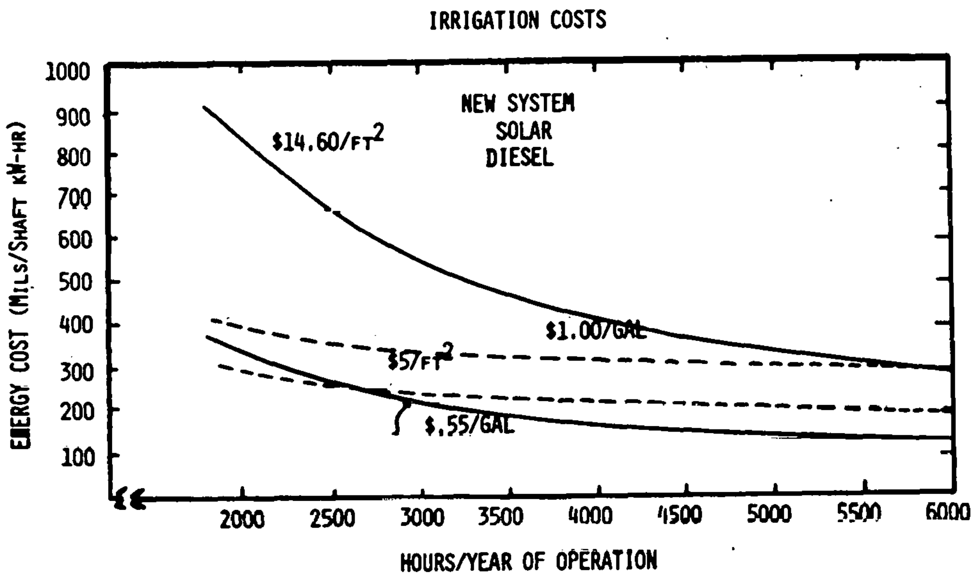


Figure 43. Economic Comparison of Solar versus Diesel Fuel for New System

The results for a new system indicated that solar with $\$5/ft^2$ collectors would compete with natural gas at $5/mcf if operated 2300 hr/yr, with 10¢/kW-hr electricity at 1500 hr/yr, and diesel at $1.00/gal initially. It will compete also with the lower cost estimated fuels in the diesel and almost compete with natural gas and electricity.

The results (Figures 39-43) indicate that solar systems must be standardized so that mass production can be possible for them to become economically competitive. There are several scenarios relative to incentives and optimizing the design that can be argued, and future system studies should indicate the correct approach for establishing solar irrigation economics.

## Status of ERDA/New Mexico Experiment

As of January 1, 1977, construction of the experiment was underway, and it was approximately 30 percent complete. Some of the construction can be seen in Figure 6. As can be seen the foundations for the collectors are complete and the pond is nearly complete. The well is drilled, the expansion tank is buried, the trailer office is on site and the electrical power is on site. Although unusually bad weather has slowed construction, it is still expected that the system will be operational by May 1, 1977, as planned.

The expanded Irrigation Program indicates this experiment will continue through 1979. This will allow operational data to be obtained on the system to determine any trends of component degradation, a test bed for design improvement ideas, and an average of agricultural results over three growing seasons. It will also allow experiments on the use of the collected energy during the non-irrigation season. This use may be important to the economic feasibility of the solar irrigation experiment.

## References


1. R. L. Alvis and J. M. Alcone, Solar Powered Irrigation System, SAND76-0358, Sandia Laboratories, Albuquerque, NM, September 1976.

2. Jerry M. Alcone, Sharla G. Vandevender, and Robert L. Alvis, Solar Irrigation Program Plan, SAND76-0594, Sandia Laboratories, Albuquerque, NM, November 1976.

3. Gordon Slogget, Energy Used for Pumping Water in the United States, 1974, Oklahoma State University, Stillwater, OK, October 1975.

4. The owner operator of the farm is Mr. Ted Schrimsher of Roswell, NM.

5. For more information, contact Dr. A. Veneruso, Sandia Laboratories, Albuquerque, NM, Phone (505) 264-9162.

6. The data was collected and tests conducted by Dr. Miller of Sandia Laboratories, Albuquerque, NM. The information exists as internal memoranda at Sandia.

7. Solar Powered Irrigation Systems, Sandia Laboratories Schedule 189, January 1976-October 1977, dated December 12, 1975.

8. Joe Abbin of Sandia Laboratories assisted in this evaluation.

9. Jack W. Reed, Wind Power Climatology of the United States, SAND74-0348, Sandia Laboratories, Albuquerque, NM, June 1975.

10. R. F. Blackwell, L. V. Feltz, and R. E. Sheldahl, Wind Tunnel Data for the Darrieus Wind Turbine with NACA-0012 Blades, SAND76-0130, Sandia Laboratories, Albuquerque, NM, May 1976.

11. Water Resource Regions and Subregions for the National Assessment of Water and Related Land Resources, Water Resources Council, Washington, DC, July 1970.

DISTRIBUTION:

US Energy Research and Development Adm. (20)
Division of Solar Energy
20 Massachusetts Avenue
Washington, DC 20545
Attn: J. Weisiger
Projects Branch

New Mexico State University (10)
Energy Res. and Development Institute
Box 3449
Las Cruces, NM 88003
Attn: R. San Martin

New Mexico State University
Mechanical Engineering College
Box 3450
Las Cruces, NM 88003
Attn: T. Mancini

New Mexico State University
Agricultural Engineering College
Box 3268
Las Cruces, NM 88003
Attn: G. Abernathy

T. Schrimsher (5)
P.O. Box 1698
Roswell, NM 88201

R. Daugherty
Torrance County Extension Agent
Estancia, NM 87016

University of New Mexico
Economics Res. Department
Albuquerque, NM 87106
Attn: Dolores Alfieri

U.S. Department of the Interior
Fish and Wildlife Service
P.O. Box 1306
Albuquerque, NM 87103
Attn: J. L. Stegman
Deputy Regional Director

South Dakota State University
Electrical Engineering Department
Brookings, SD 57006
Attn: W. E. Knabach, Professor

The Aerospace Corporation
Bldg C-101, Rm 690
P.O. Box 92957
Los Angeles, CA 90009
Attn: A. Latta

Solar Systems West
421 Court Street
Elko, NV 80801
Attn: Shelly Gordon

Dell Laboratories
Rm HE009
Whippany, NJ 07981
Attn: S. Fineblum

Bonneville Power Administration
P.O. Box 3621
Portland, OR 97208
Attn: D. Hartman (EOB)

Acurex Corporation (8)
485 Clyde Avenue
Mountain View, CA 94042
Attn: R. R. Malone/SAO (2)
P. Grace ERDA/ALO (5)
G. Neuner (1)

Black & Veatch Consulting Engineers
1500 Meadow Lake Parkway
Kansas City, MO 64114
Attn: J. K. Kintigh

Honeywell Corporation
Energy Resources Center
2600 Ridgeway Parkway
Minneapolis, MN 55413
Attn: D. Evans

Tri-State Generation & Transmission
Association, Inc.
P.O. Box 29198
Denver, CO 80229
Attn: P. Swanson

Federal Energy Administration
Box 2208
Kansas City, MO 64112
Attn: G. Wenzel

Pechiney Development
825 Third Avenue
New York, NY 10022
Attn: Linda Lubitz

Intercon Research Associates, Ltd.
1219 Howard Street
Evanston, IL 60202
Attn: Rosemary D. Killumann

Utah Power & Light
P.O. Box 899
Salt Lake City, UT 84110
Attn: K. Evans

Public Service Company
P.O. Box 2267
Albuquerque, NM 87103
Attn: M. Lechner

DISTRIBUTION: (cont)

Texas A & M University
Agricultural Engineering Department
College Station, TX 77843
Attn: W. Le Pori

F. Bartels
12160 Clarelta Street
Lakeview Terrace, CA 91342

Battelle-Pacific Northwest Laboratory
P.O. Box 999
Richland, WA 99352
Attn: A. Fassbender

Irrigation & Industrial Development Corp.
260 Madison Avenue
New York, NY 10016
Attn: F. L. Jamison, Manager

Battelle Memorial Institute
Columbus Laboratories
505 King Avenue
Columbus, OH 43201
Attn: P. Hofmann
Associate Director, Energy Programs

| | |
|---|---|
| 2324 | L. W. Schulz |
| 2324 | J. P. Abbin |
| 5000 | A. Narath |
| 5700 | J. H. Scott |
| 5715 | R. H. Braasch (200) |
| 5715 | R. L. Alvis |
| 5740 | V. L. Dugan |
| 5742 | S. G. Varnado |
| 5742 | S. Vandevender |
| 8266 | E. A. Aas (2) |
| 3141 | C. A. Pepmueller (Actg) (5) |
| 3151 | W. L. Garner (3) |
| | For ERDA/TIC (Unlimited Release) |

ERDA/TIC (25)
(R. P. Campbell, 3171-1)